NOAA Technical Memorandum NESS 81

# ESTIMATION OF DAILY PRECIPITATION OVER CHINA AND THE USSR USING SATELLITE IMAGERY

Washington, D.C.
September 1976

noaa NATIONAL OCEANIC AND ATMOSPHERIC ADMINISTRATION / National Environmental Satellite Service

Nati[illegible] Service Series

The National Environmental Sate[illegible]rvice (NESS) is responsible for the establishment and operation of the environmental satellite systems of NOAA.

NOAA Technical Memorandums facilitate rapid distribution of material that may be preliminary in nature and so may be published formally elsewhere at a later date. Publications 1 through 20 and 22 through 25 are in the earlier ESSA National Environmental Satellite Center Technical Memorandum (NESCTM) series. The current NOAA Technical Memorandum NESS series includes 21, 26, and subsequent issuances.

Publications listed below are available from the National Technical Information Service, U.S. Department of Commerce, Sills Bldg., 5285 Port Royal Road, Springfield, Va. 22151. Prices on request. Order by accession number (given in parentheses). Information on memorandums not listed below can be obtained from Environmental Data Service (D831), 3300 Whitehaven St., NW., Washington, D.C. 20235.

NESS 41 Effect of Orbital Inclination and Spin Axis Attitude on Wind Estimates From Photographs by Geosynchronous Satellites. Linwood F. Whitney, Jr., September 1972, 32 pp. (COM-72-11499)

NESS 42 Evaluation of a Technique for the Analysis and Forecasting of Tropical Cyclone Intensities From Satellite Pictures. Carl O. Erickson, September 1972, 28 pp. (COM-72-11472)

NESS 43 Cloud Motions in Baroclinic Zones. Linwood F. Whitney, Jr., October 1972, 6 pp. (COM-73-10029)

NESS 44 Estimation of Average Daily Rainfall From Satellite Cloud Photographs. Walton A. Follansbee, January 1973, 39 pp. (COM-73-10539)

NESS 45 A Technique for the Analysis and Forecasting of Tropical Cyclone Intensities From Satellite Pictures (Revision of NESS 36). Vernon F. Dvorak, February 1973, 19 pp. (COM-73-10675)

NESS 46 Publications and Final Reports on Contracts and Grants, 1972. NESS, April 1973, 10 pp. (COM-73-11035)

NESS 47 Stratospheric Photochemistry of Ozone and SST Pollution: An Introduction and Survey of Selected Developments Since 1965. Martin S. Longmire, March 1973, 29 pp. (COM-73-10786)

NESS 48 Review of Satellite Measurements of Albedo and Outgoing Long-Wave Radiation. Arnold Gruber, July 1973, 12 pp. (COM-73-11443)

NESS 49 Operational Processing of Solar Proton Monitor Data. Louis Rubin, Henry L. Phillips, and Stanley R. Brown, August 1973, 17 pp. (COM-73-11647/AS)

NESS 50 An Examination of Tropical Cloud Clusters Using Simultaneously Observed Brightness and High Resolution Infrared Data From Satellites. Arnold Gruber, September 1973, 22 pp. (COM-73-11941/4AS)

NESS 51 SKYLAB Earth Resources Experiment Package Experiments in Oceanography and Marine Science. A. L. Grabham and John W. Sherman, III, September 1973, 72 pp. (COM 74-11740/AS)

NESS 52 Operational Products From ITOS Scanning Radiometer Data. Edward F. Conlan, October 1973, 57 pp. (COM-74-10040)

NESS 53 Catalog of Operational Satellite Products. Eugene R. Hoppe and Abraham L. Ruiz (Editors), March 1974, 91 pp. (COM-74-11339/AS)

NESS 54 A Method of Converting the SMS/GOES WEFAX Frequency (1691 MHz) to the Existing APT/WEFAX Frequency (137 MHz). John J. Nagle, April 1974, 18 pp. (COM-74-11294/AS)

NESS 55 Publications and Final Reports on Contracts and Grants, 1973. NESS, April 1974, 8 pp. (COM-74-11108/AS)

NESS 56 What Are You Looking at When You Say This Area Is a Suspect Area for Severe Weather? Arthur H. Smith, Jr., February 1974, 15 pp. (COM-74-11333/AS)

NESS 57 Nimbus-5 Sounder Data Processing System, Part I: Measurement Characteristics and Data Reduction Procedures. W.L. Smith, H. M. Woolf, P. G. Abel, C. M. Hayden, M. Chalfant, and N. Grody, June 1974, 99 pp. (COM-74-11436/AS)

NESS 58 The Role of Satellites in Snow and Ice Measurements. Donald R. Wiesnet, August 1974, 12 pp. (COM-74-11747/AS)

(Continued on inside back cover)

NOAA Technical Memorandum NESS 81

# ESTIMATION OF DAILY PRECIPITATION OVER CHINA AND THE USSR USING SATELLITE IMAGERY

Walton A. Follansbee

Washington, D.C.
September 1976



UNITED STATES
DEPARTMENT OF COMMERCE
Elliot L. Richardson, Secretary

NATIONAL OCEANIC AND
ATMOSPHERIC ADMINISTRATION
Robert M. White, Administrator

National Environmental
Satellite Service
David S. Johnson, Director

CONTENTS

# ESTIMATION OF DAILY PRECIPITATION OVER CHINA AND THE USSR USING SATELLITE IMAGERY

Walton A. Follansbee
National Environmental Satellite Service, NOAA, Washington, D.C.

ABSTRACT. This memorandum describes a technique for estimating precipitation over China and the USSR in late autumn, winter, and early spring, using satellite data. The data consisted of NOAA-4 infrared imagery taken at approximately 9 a.m. and 8 p.m., local time, and visual pictures taken near 9 a.m. local time, all with one-half mile resolution. The major human input to the technique is identification of precipitating clouds in the infrared imagery, aided by inspection of the visual pictures.

The technique consists of three steps: (1) delineate the area(s) covered by precipitating clouds in each of two consecutive infrared images taken at approximately 12-hour intervals; (2) using cloud motion models developed for the purpose, delineate the envelope of precipitation and isopleths of duration of precipitation in hours; (3) using an empirically derived relationship between duration of precipitation and the percentage of monthly normal precipitation, estimate amounts of precipitation for the 12-hour period at each grid point in the area of interest. The relationship is $P_{12} = 0.0075\ DP_N$, where D is duration in hours, $P_N$ is monthly normal precipitation, and $P_{12}$ is total precipitation in the 12-hour period.

Satellite data for the period November 21, 1974, to February 28, 1975, were used to develop the technique and to establish the relationships. The technique was then tested in a quasi-operational mode for the months of March and April, 1975. For March 1975, the ratio of total error to total observed precipitation for the USSR was 0.55, and the ratio of algebraic error to total observed precipitation was 0.01. This degree of accuracy and the absence of significant bias was repeated in the April estimates for the USSR. A similar test over 24 States in the central United States for April 1976 gave ratios of 0.46 and -0.28. This underestimate is due largely to frequent thunderstorms over the U.S. in April 1976.

## INTRODUCTION

The problem of estimating precipitation using satellite data has received increasing attention by a number of investigators in recent years. To date the emphasis has been on convective rain over the tropics and in summer in the subtropics, usually for mesoscale areas.

The technique described herein was prompted by the need for estimting precipitation over vast agricultural regions of Asia in autumn, winter, and spring. Convective rain is far less prevalent in these Asiatic areas during the colder months than in regions investigated in previous studies. This has both advantages and disadvantages. Except in well-defined frontal systems, nimbostratus is more difficult to identify than cumulonimbus. On the other hand, precipitation from nimbostratus is far more uniformly distributed than that from cumulonimbus.

## ASSUMPTIONS

An examination of climatological records led to the assumption that, in a normal month over the middle latitudes of Asia, two storms per week or nine storms per month could be expected. If the storms were of uniform intensity, each might contribute 11% of the monthly normal precipitation. Assuming that 11% fell in a 24-hour day, about 6% could be expected in a 12-hour period, provided the precipitation was continuous throughout the 12 hours. An analysis of the data showed that for a given point the duration of precipitation is usually less than 24 hours, suggesting that normally more than 6% would occur in a continuous 12-hour rain or snow period.

In the interest of simplicity, the precipitation rate in all parts of a rain cloud has been considered constant in most cases, especially during the development of the technique. On the other hand, it is assumed that an experienced satellite meteorologist will have the capability of determining, in most cases, which clouds or parts of clouds are in fact precipitating, and at times, of assigning different intensities to various parts of the cloud.

## CLOUD MOTION MODELS

While it is usually not difficult to identify a precipitating cloud mass in succeeding 12-hour pictures, the duration of precipitation along its path during the 12 hours presents problems. Motion models were developed to cope with these problems.

One of the simplest of such models would be a rectangular cloud with major axis oriented north-south, moving from west to east at uniform speed, and traveling in 12 hours a distance equal to its minor axis, without changing shape or size. That is, at the end of 12 hours its trailing edge will reach a line occupied by the leading edge at the beginning of the 12-hour period, as shown in figure 1. Let us assume that the cloud is 100 miles long and 60 miles wide, and the satellite pictures have been taken at midnight and noon on a given day. Then at 2 a.m. the trailing edge of the cloud will have

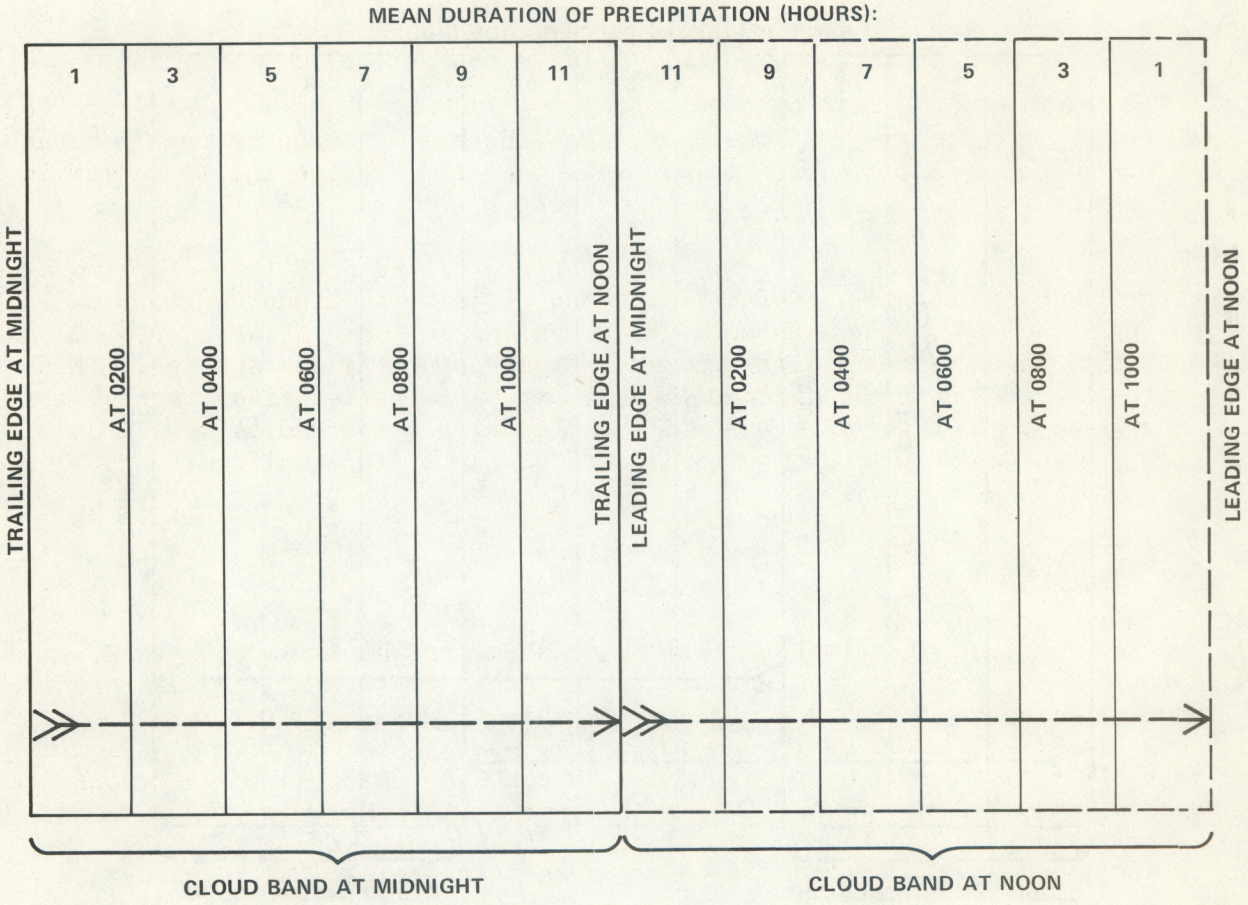


Figure 1.--Cloud motion model, case 1. Rectangular, no overlap or underlap

moved 10 miles east of its midnight position, and a strip 10 miles by 100 miles will have cleared. Precipitation will have ended at midnight along the western edge of this strip but will end at 2 a.m. along the eastern edge; therefore the average duration of precipitation within the entire strip will be 1 hour. But during this period all of the area extending 50 miles east of the strip will have received precipitation throughout the 2 hours. In the same way it can be shown that between 2 and 4 a.m. the 10-mile wide strip immediately east of this first strip will have an average duration of 1 hour, for a total of 3 hours duration from midnight to 4 a.m. Likewise, the next strip to the east will have an average duration of 5 hours, and the next three strips will have 7, 9, and 11 hours, respectively.

In like manner, following the progress of the leading edge of the cloud mass, we see there would be six more strips 10 miles wide with average duration values in hours of 11, 9, 7, 5, 3, and 1, decreasing eastward.

A second case, shown in figure 2, is similar to the first, but traveling in 12 hours a distance equal to twice its minor axis. At this speed, it can be shown that duration of precipitation will not exceed 6 hours at any point

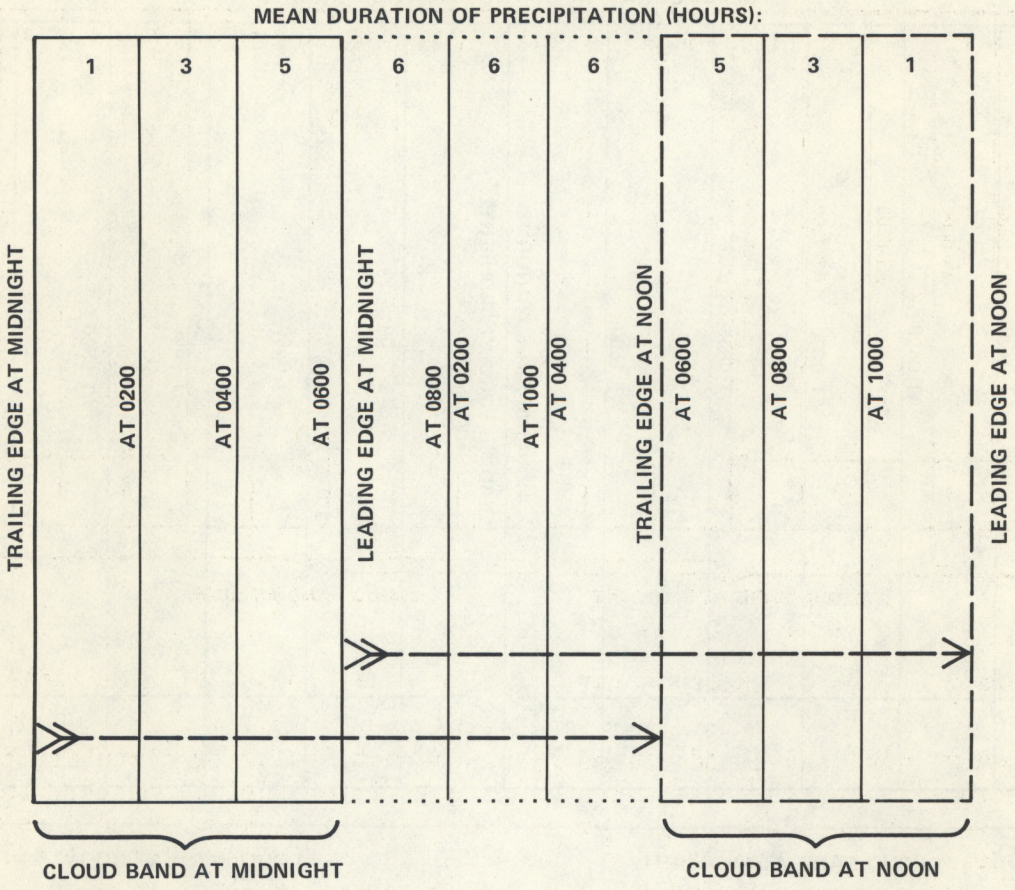


Figure 2.--Case 2. Rectangular, underlap equal to width of band.

along the cloud's track. This case has an underlap* equal to the width of the cloud band, or the cloud band's minor axis.

Figure 3 presents a third case of a rectangular cloud, moving in the direction of its major axis a distance of half the length of the major axis in 12 hours. This case provides a 50% overlap of the original cloud position and the cloud position 12 hours later. If the major axis is 120 miles and the minor axis 100 miles, the entire envelope of precipitation will be the perimeter of a rectangle 100 by 180 miles. If, as before, the cloud is moving from west to east, we could divide the entire precipitation area into 18 rectangular strips 10 miles wide and 100 miles long, such that the average duration of precipitation in hours, beginning with the westernmost and ending with the easternmost strip, would be 1, 3, 5, 7, 9, 11, 12, 12, 12, 12, 12, 12, 11, 9, 7, 5, 3, and 1.

Figure 4 shows cases similar to cases 1, 2, and 3, but for circular cloud masses rather than rectangular.

---

*Underlap=the distance between the leading edge of the cloud mass at initial time and the trailing edge of the same cloud mass at the end of the time period under consideration.

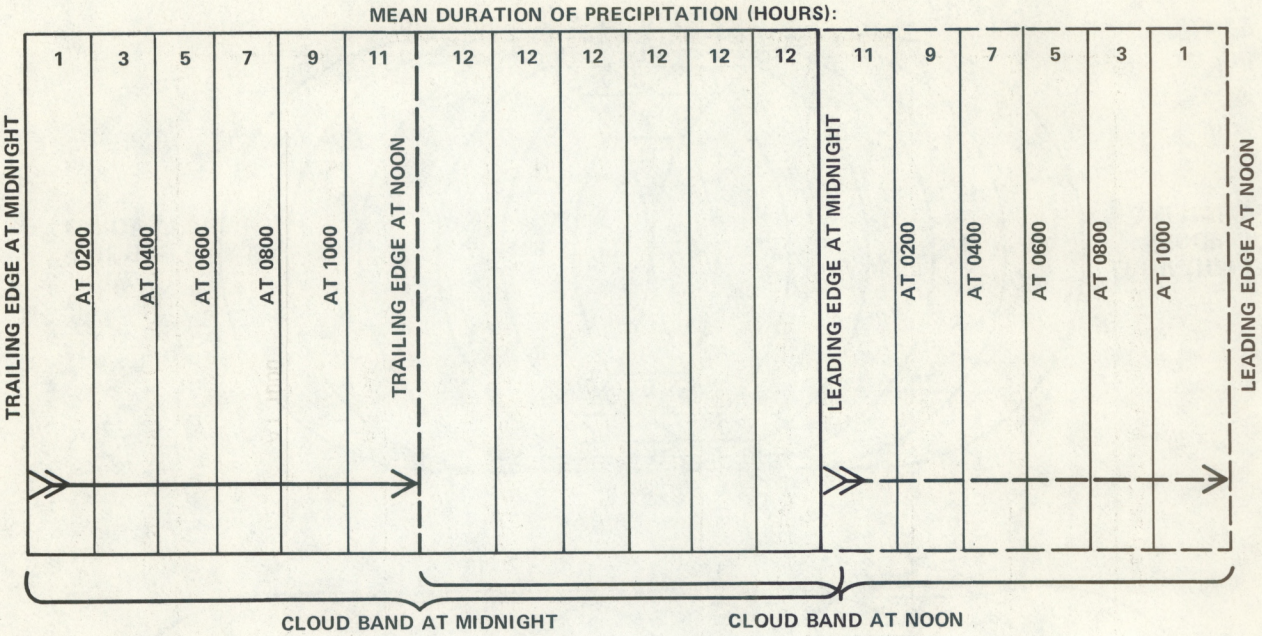


Figure 3.--Case 3. Rectangular, overlap equal to 50% of band width.

Obviously, not many cloud masses retain a rectangular or circular shape of uniform size for 12 consecutive hours. It is possible, however, to adapt cases 1 through 6, singly or in combination, to many cloud masses as they appear in satellite imagery. Figure 5 shows a somewhat idealized frontal system moving uniformly with little change in shape or size. The upper third is fairly circular and shows approximately 50% overlap; therefore it may be treated like case 6. The middle third is fairly rectangular, with little overlap or underlap, and may be likened to case 1. The lower third remains nearly rectangular and averages an underlap approximately equal to its width; thus it may be treated like case 2. The isopleths of precipitation duration have been smoothed in regions of transition from one case to the next.

Figure 6 shows examples of three cloud systems, cases 8, 9, and 10, which either expand or contract without any other lateral motion. The concentric isopleths of precipitation duration are drawn the same way regardless of whether the system is contracting or expanding.

Figure 7a shows a slightly more complex but more realistic motion pattern, case 11. The cloud band is diminishing as it moves along a diagonal. Positions are shown at 3-hour intervals beginning at 0000, ending at 1200 hours. Beginning and ending times of precipitation are indicated for various points and lines. Based on these and additional beginnings and endings (not shown), isopleths of duration of precipitation are outlined in figure 7b.

The underlap in case 11 is approximately equal to the width of the cloud band at initial time. Case 12, figure 8a, is similar to case 11 except that there is a small overlap equal to one-third of the cloud band width at final

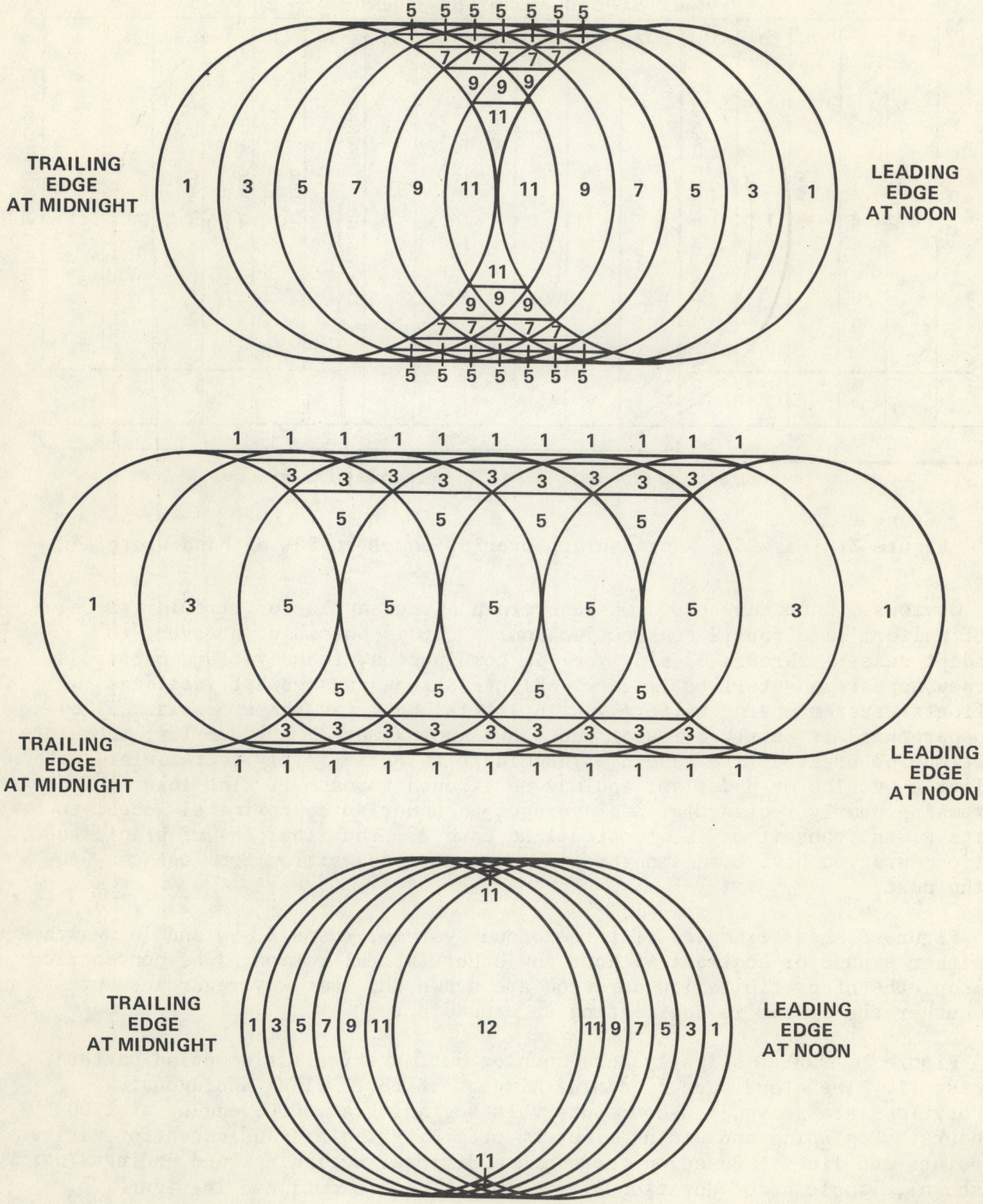


Figure 4.--Circular cloud motion models. *Top:* Case 4, no overlap or underlap at line of centers. *Center:* Case 5, underlap at line of centers equal to diameter. *Bottom:* Case 6, 50% overlap along line of centers.

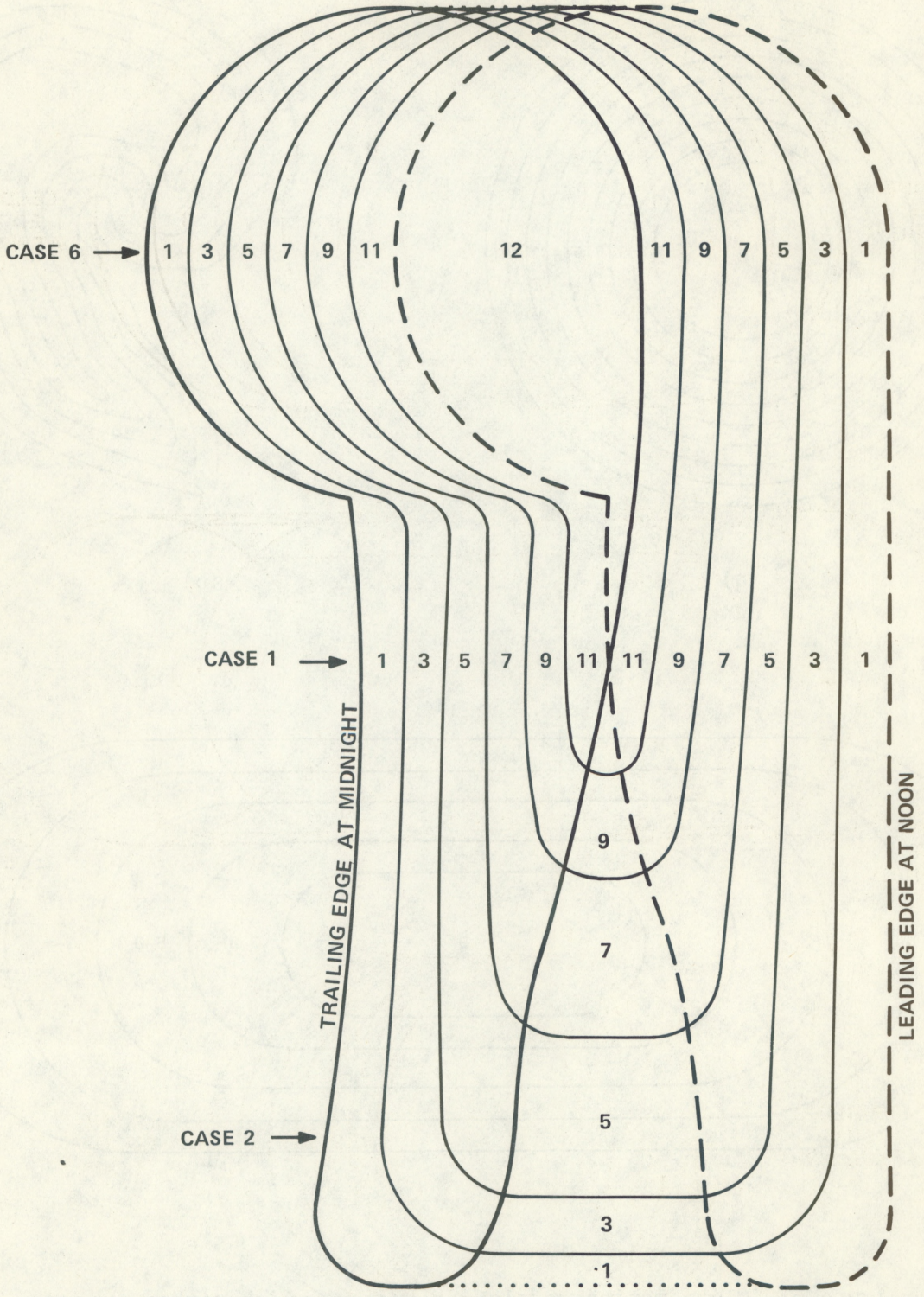


Figure 5.--Case 7. Composite cloud motion model, combining cases 1, 2, and 6.

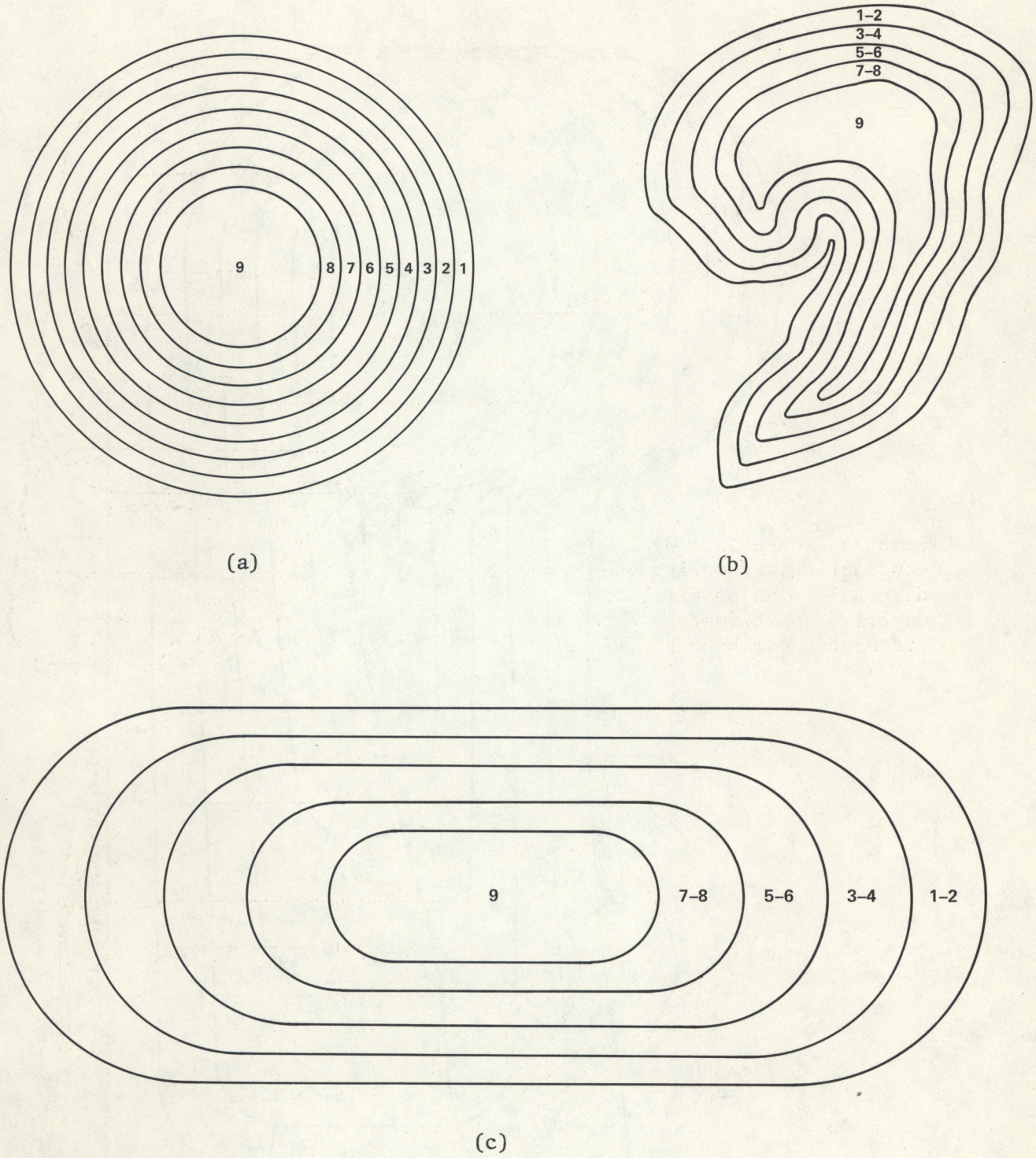


Figure 6.--Cloud motion models for systems which either expand or contract without any other lateral motion. (a) Case 8, circular; (b) Case 10, vortical; (c) Case 9, oval.

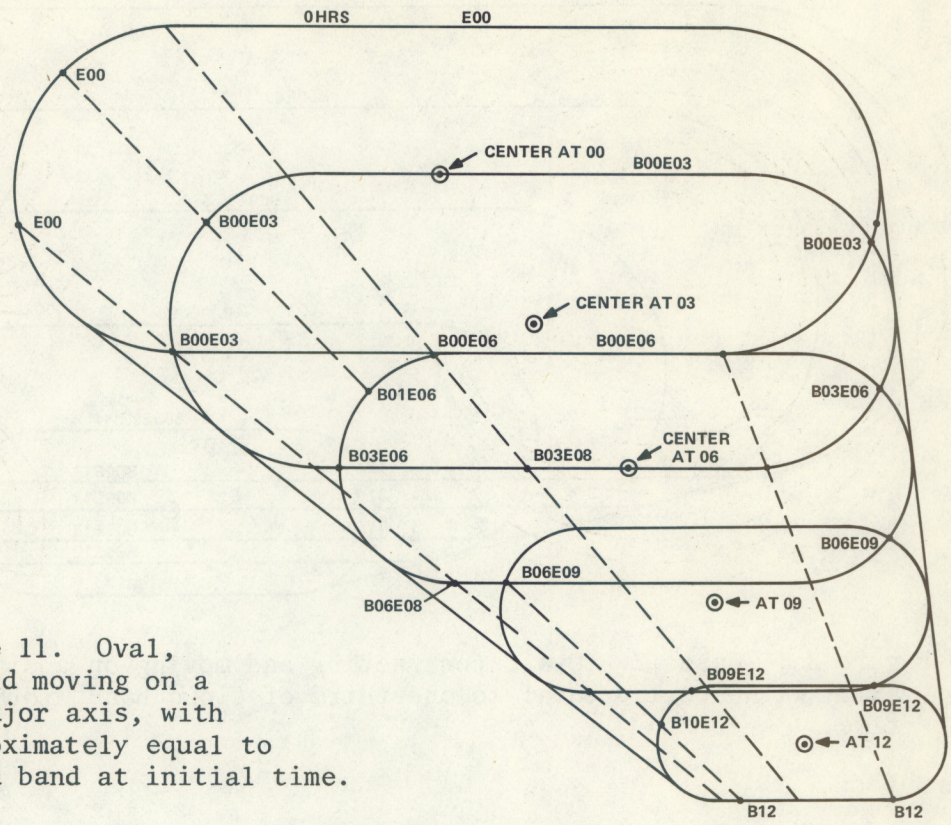


Figure 7a.--Case 11. Oval, contracting and moving on a diagonal to major axis, with underlap approximately equal to width of cloud band at initial time.

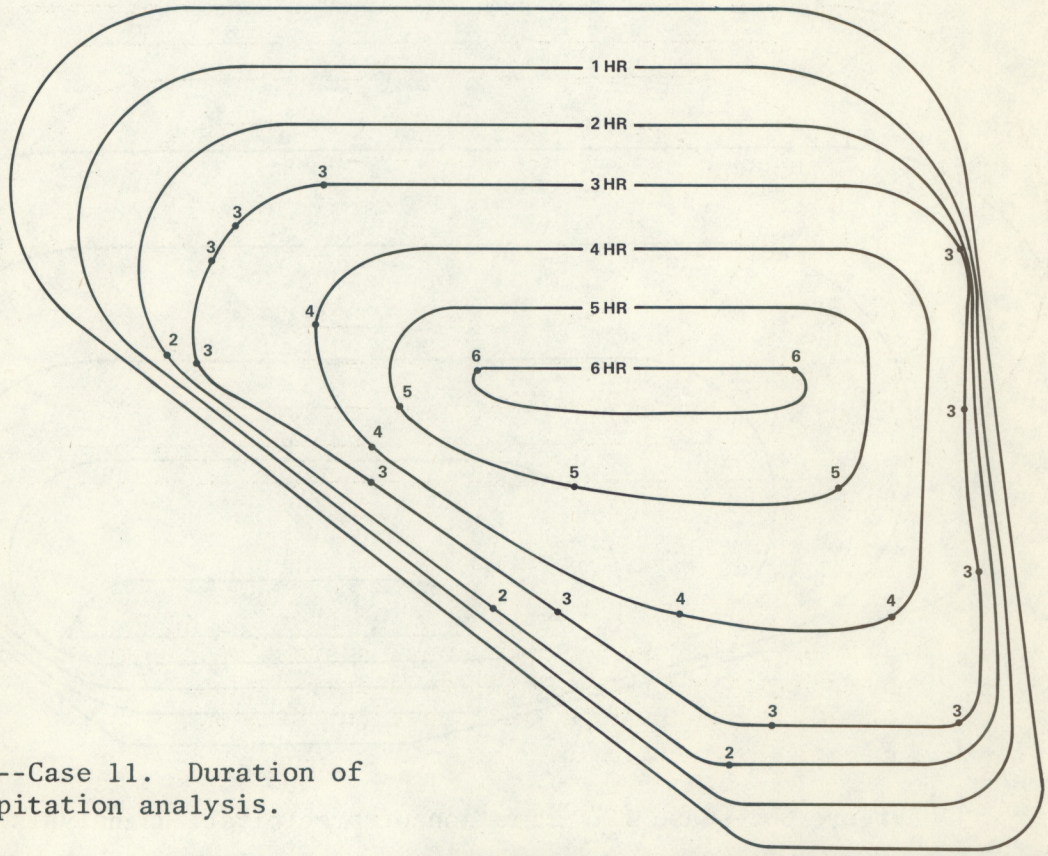


Figure 7b.--Case 11. Duration of precipitation analysis.

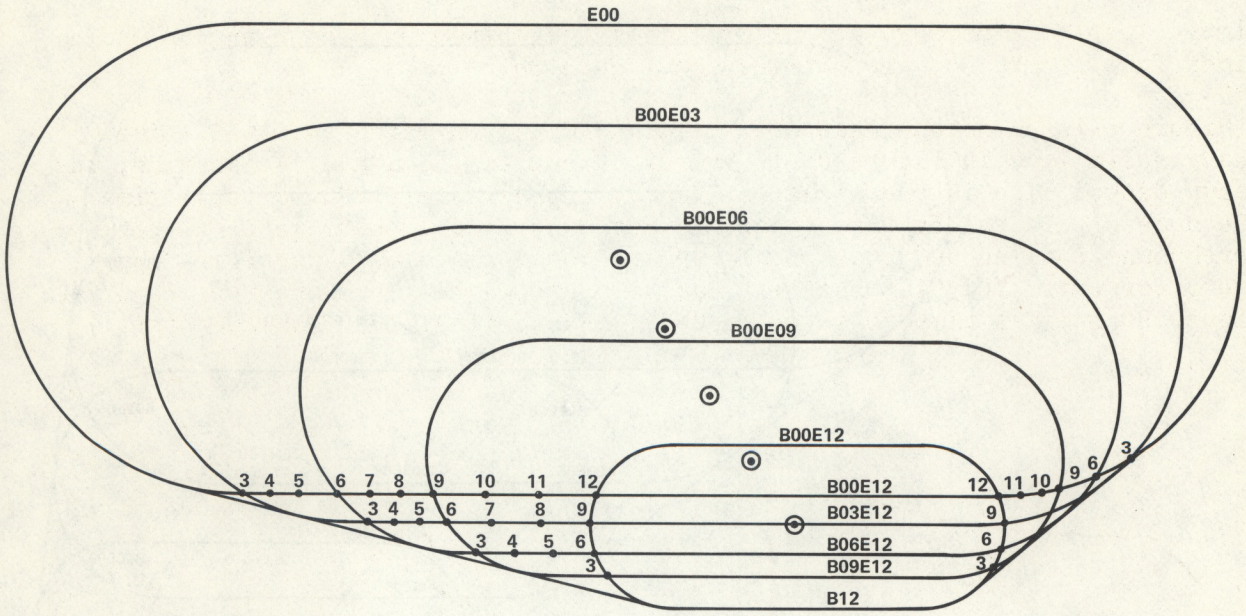


Figure 8a.--Case 12. Oval, contracting and moving on a diagonal to major axis, with overlap equal to one-third of cloud band width at terminal time.

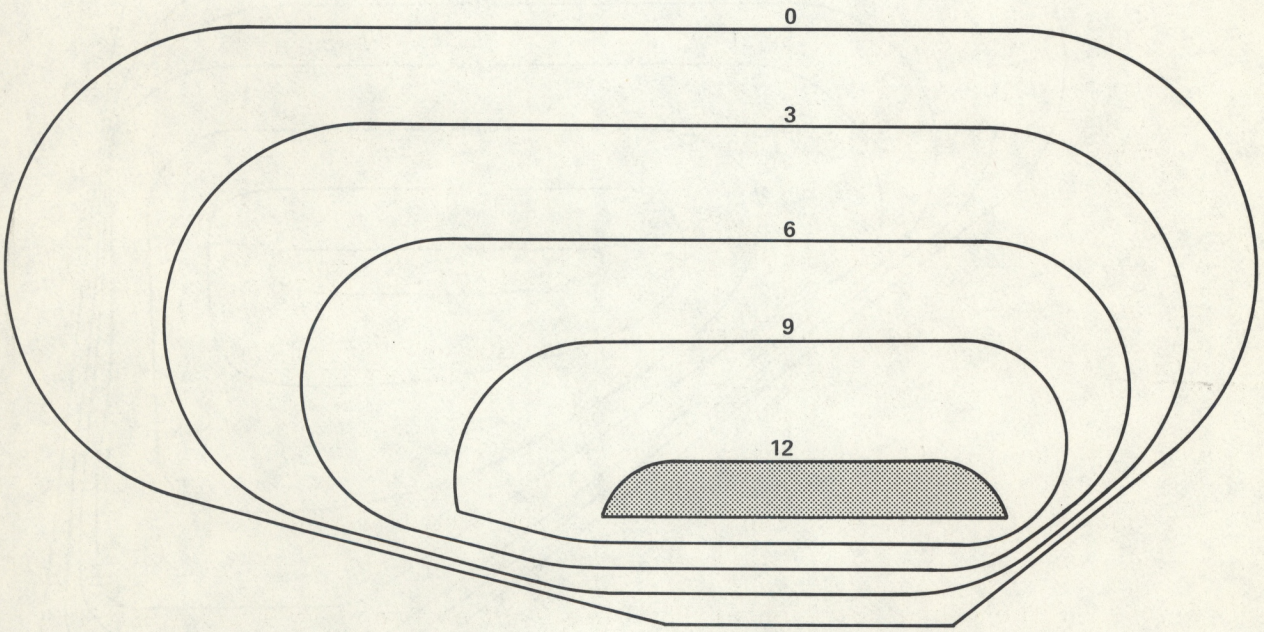


Figure 8b.--Case 12. Duration of precipitation analysis.

time. Isopleths of duration of precipitation, based on beginning and ending times from figure 8a, are outlined on figure 8b.

Figure 9 is an actual case over mainland China on March 14, 1975. The heavy solid line in figure 9a is the cloud outline at 9 a.m. local time; the heavy dashed line is the cloud outline at approximately 8 p.m. local time. (Because of orbital factors, there is not exactly a 12-hour interval between northbound morning and southbound evening local picture-taking time. However, for this study the interval has been assumed to be 12 hours. Thus for figure 9b, initial time is given as 0000, and terminal time as 1200 hours.)

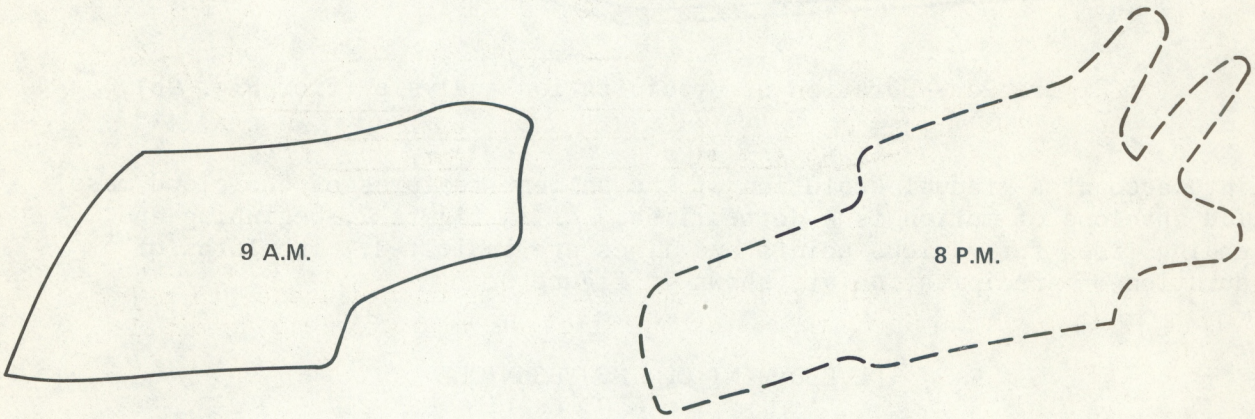


Figure 9a.--Cloud positions over China at 9 a.m. and 8 p.m. local time, March 14, 1975.

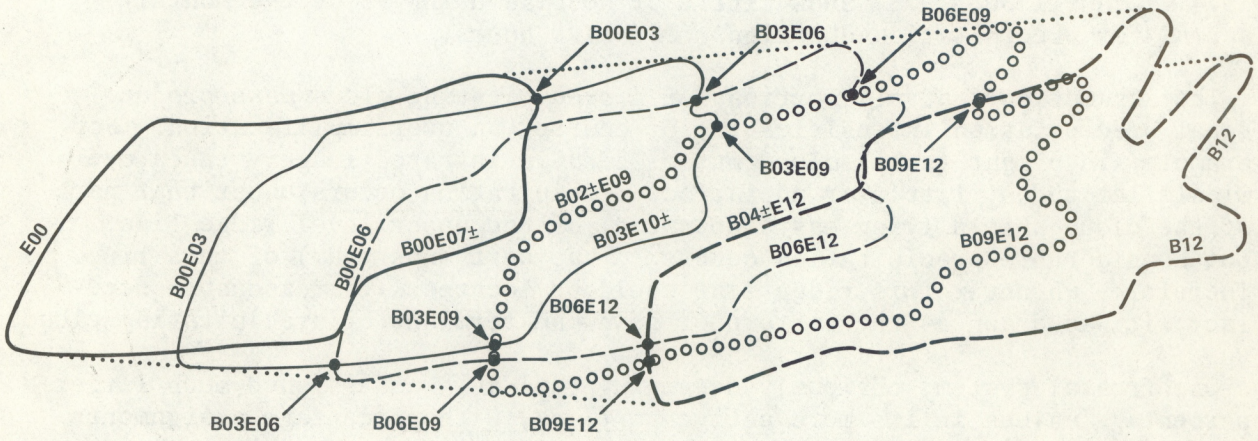


Figure 9b.--Cloud positions at 3-hour intervals (from Fig. 9a).

In figure 9b the cloud position at 0300 hours is outlined in a light solid line; at 0600 hours, in a light dashed line; and at 0900 hours, in a line of small circles. These intermediate positions have been "eyeballed," taking

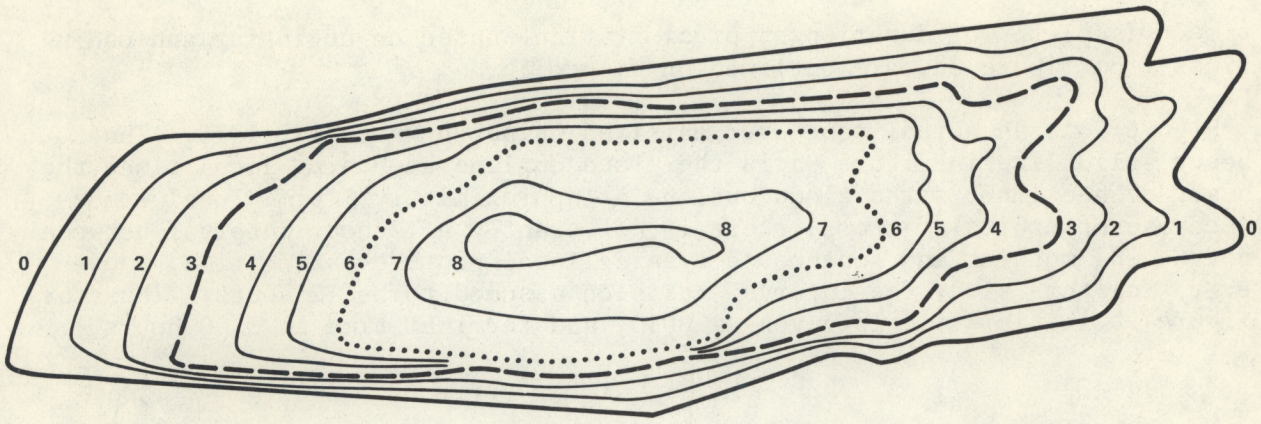


Figure 9c.--Duration of precipitation analysis (from Fig. 9b).

into account a gradual evolution of the salient features of the cloud mass. The envelope of motion is a dotted line. As in figure 7, beginning and ending times for various points and lines are indicated. Isopleths of duration of precipitation are shown in figure 9c.

## DEVELOPMENT OF THE TECHNIQUE

The original assumption, that a point remaining under a precipitating cloud for 12 hours should produce 6% of the monthly normal for that point, was tested over the USSR for late November and early December 1974. When this resulted in general underestimates, the figure was raised to 12%. This produced overestimates of comparable magnitude. The figure ultimately adopted was 9%. All subsequent tests, covering the period from November 24, 1974, to April 30, 1975, show little or no bias using 9% of the monthly normal for precipitation durations of twelve hours.

The assumption that all portions of a precipitating cloud mass produce equal precipitation intensities is, of course, an oversimplification. For example, in bright (cold) cloud masses seen in infrared imagery taken over middle latitudes, little or no surface precipitation occurs under that part of the cloud shield lying east (downwind) of the upper level ridge line, but considerable precipitation occurs to the west (upstream) of this line. Therefore, whenever this ridge line could be located with reasonable accuracy, it was drawn as the eastern or downwind terminus of precipitating cloud.

One frontal system, obviously deepening rapidly, was assigned much larger percentage values in its more active portions, with percentage assignments tapering off toward the storm periphery.

In general, precipitation was considered less intense near the lateral edges of the cloud mass--for example, near the northern and southern edges of a system moving eastward. It seemed unwise, however, in the early stages of the investigation and development, to introduce too much subjective judgment. Therefore, with the above-mentioned exceptions, the rule adopted was to assign equal intensities to all parts of a precipitating cloud.

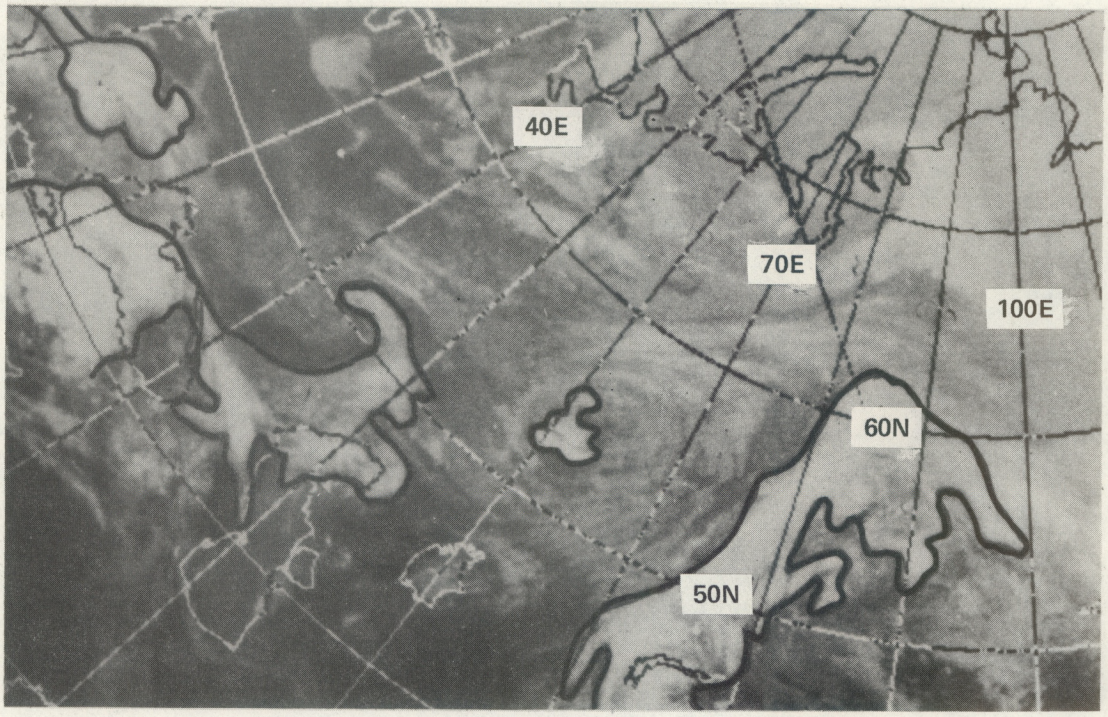


Figure 10.--Infrared imagery taken at approximately 9 a.m., local time, March 22, 1975, over Asia.

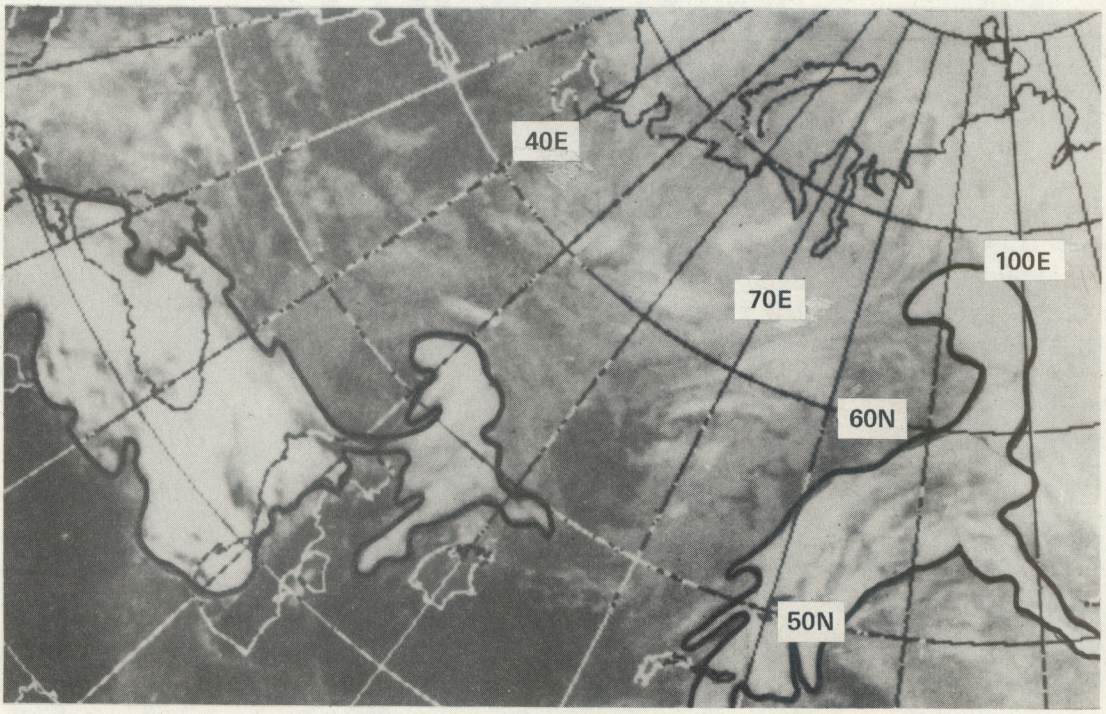


Figure 11.--Infrared imagery taken at approximately 8 p.m., local time, March 22, 1975, over Asia.

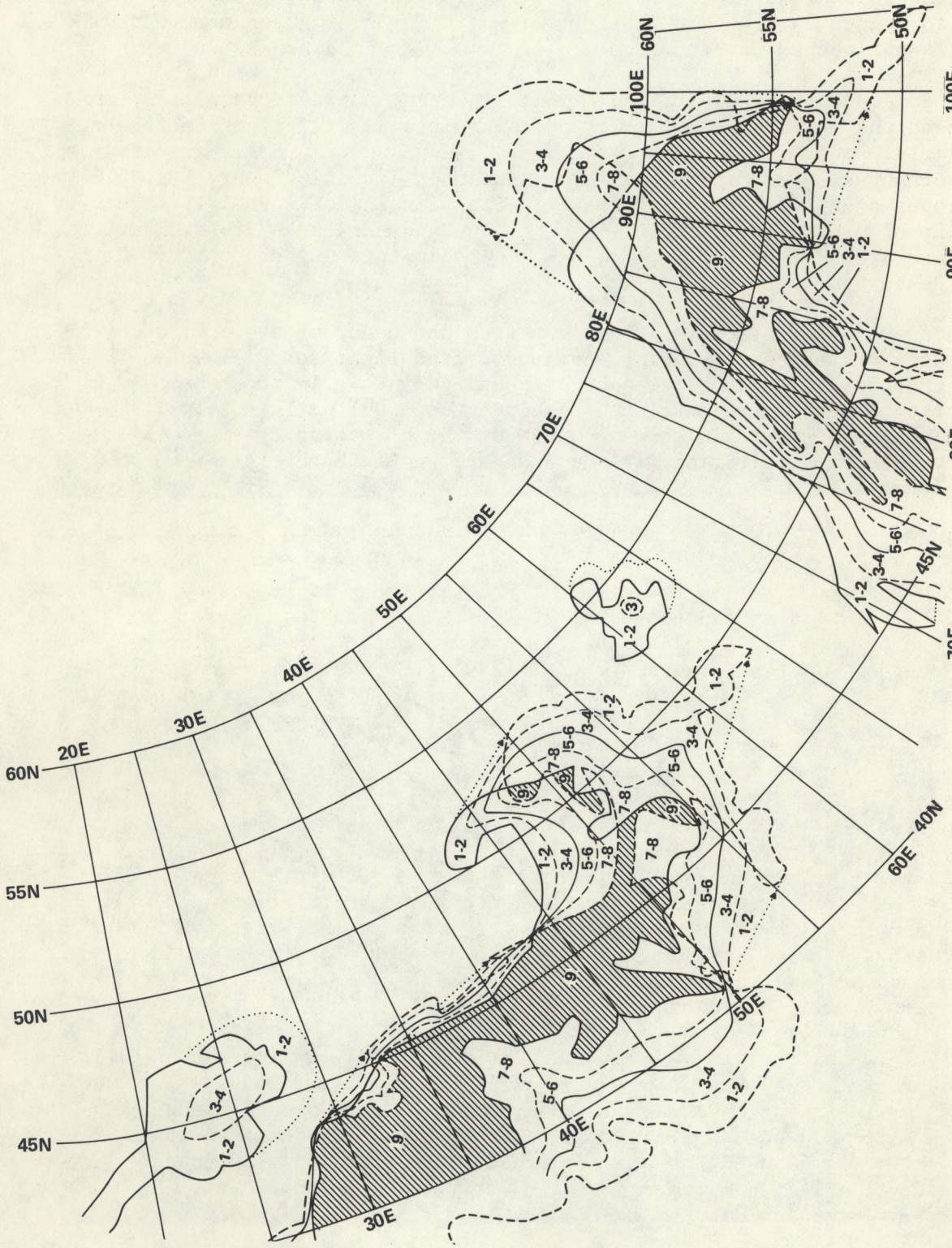


Figure 12.--Workmap, USSR, for the period 9 a.m. to 8 p.m., local time, March 22, 1975.

## PROCEDURE

An understanding of the procedure finally adopted is facilitated by reference to figure 12, the workmap for estimating precipitation over the USSR for the period, 9 a.m. to 8 p.m. local time, March 22, 1975.

The outlines of precipitating clouds at 9 a.m., seen in figure 10, are drawn on the workmap in any selected color (heavy solid lines in figure 12). Similarly, precipitating clouds at 8 p.m., seen in figure 11, are drawn on the workmap in a different color (heavy dashed lines in figure 12). The envelopes of cloud motion are drawn (dotted lines in figure 12). Areas of overlap of precipitating clouds are shaded, and marked "9" to indicate that in these areas 9% of the monthly normal precipitation is occurring during the 12-hour period.

Lines are drawn bisecting the zones from the edges of the overlap areas to the edges of the corresponding envelopes. The light solid lines, such as that crossing 40°N, 40°E, are such bisecting lines. In zones bounded by the bisecting line and the envelope, precipitation will be less than 4.5% of the monthly normal, while in zones bounded by the bisecting line and the edge of the overlap, precipitation will be greater than 4.5% but less than 9% of the monthly normal.

All of these smaller zones are bisected in turn, and marked 1-2, 3-4, 5-6, and 7-8, as appropriate, to indicate sub-zones receiving 1 to 2% of the monthly normal, 3 to 4%, 5 to 6%, and 7 to 8%. The light dashed line crossing 50°N, 75°E is an example of lines separating sub-zones receiving 1 to 2% from those receiving 3 to 4% of the monthly normal. The light dashed line through 50°N, 77°E separates sub-zones having 5 to 6% from sub-zones having 7 to 8%. When desirable, these sub-zones may be bisected to delineate areas each averaging 1, 2, 3, 4, 5, 6, 7, or 8% of the monthly normal, but usually this is unnecessary.

The assignment of exact integers to these zones is somewhat arbitrary, since it can be shown that the exact means for zones designated 1, 2, 3, 4, 5, 6, 7, and 8% are, respectively, 0.56, 1.69, 2.81, 3.94, 5.06, 6.19, 7.31, and 8.44%. The absolute mean "error" is 0.25%, but the algebraic "error" is zero. The advantages of using whole numbers and exact bisections of the zones far outweigh any advantages resulting from a more rigorous but unwieldy treatment. No real error can be determined; the relationship used herein, between duration of precipitation and percent of monthly normal precipitation, is entirely empirical, hence arbitrary.

In some situations no overlap occurs during the 12-hour period. In others, the weak systems observed must be assigned less intense rainfall rates. At times an old system moves out of an area and is replaced by a new system moving into the vacated area 12 hours later. Each of these cases is exemplified in figure 13, which shows cloud motions over mainland China for the period 9 a.m. to 8 p.m., March 10, 1975. Figures 14 and 15 are the infrared imagery for this period.

In figure 13, the system moving off the coast between 26° and 37°N at 8 p.m. (the heavy dashed line) has been formed by the merging of

three smaller systems farther west at 9 a.m. (heavy solid lines). Advection is sufficiently rapid that none of these smaller clouds overlaps the 8 p.m. boundary of the merged system. The small cloud near 31°N between 113° and 119°E almost overlaps; therefore an isopleth enclosing a zone of 7% of the monthly normal is drawn from the nose of the small morning cloud well into the larger evening cloud. Zones ranging from 6% down to 1% encircle the 7% zone, out to the cloud motion envelope. The small cloud located south of 30°N at 9 a.m. fails to overlap by an even larger distance; therefore the wettest zone connecting it to the 8 p.m. cloud mass shows a mere 5% of monthly normal. Note how the isopleths are drawn between the two areas of merging. The treatment is somewhat subjective, but is considered logical.

The small cloud system along 35°N from 98° to 112°E at 9 a.m. (in figure 13) presents three special problems: (1) it moves rapidly and thus shows even greater underlap than its two companions; (2) it is weak and must be assigned less intense precipitation; and (3) as it moves rapidly eastward it is replaced by a new larger system whose nose reaches as far east as 32°N, 115°E by 8 p.m. Had this new system not moved in, the small band along 35°N at 9 a.m. would have shown 1% of the monthly normal precipitation throughout its length, except in its eastern extremity where a 2% zone connects it with the 8 p.m. position farther east. The increasing strength of the cloud with time makes it advisable to draw a small 4% zone along 35°N between 116° and 118°E. Meanwhile the new large system moving in from west of 100°E is drawn with intensities ranging from 1% to 5%. However, when the new system moves into areas previously occupied by the small weak system, graphical addition is used to show larger percentages, or greater total rainfall.

The system in extreme northeastern China in figure 13 is weakening with time. Thus the overlap area is restricted to 7% of the monthly normal rather than the usual 9%.

When percentages have been assigned to all precipitation areas, the percentage value at each grid point is multiplied by that grid point's monthly normal precipitation to obtain the estimated 12-hour precipitation. Or, if the weekly precipitation estimate is required for each grid point, percentages at the grid points may be entered on data sheets such as that shown in figure 16. Percentages for each of the fourteen consecutive 12-hour periods of the week are entered on the fourteen numbered lines. Grid point numbers appear at the head of each column. The total for each column is multiplied by the grid point normal for the month to get the precipitation estimate for the week. Alternatively, once the map has been completed, the grid point data may be scanned and stored by computer for subsequent retrieval.

## TESTS AND VERIFICATION

The method was tested in a quasi-operational mode for the USSR and mainland China for the period March 1 to April 30, 1975. The author made twice-daily estimates of precipitation for 660 Russian and 450 Chinese grid points, summed these to get weekly precipitation estimates at each grid point, and drew isohyetal analyses of the estimates for each week of the period. The estimates for March 1975 were begun on March 4, 1975 (when the first imagery

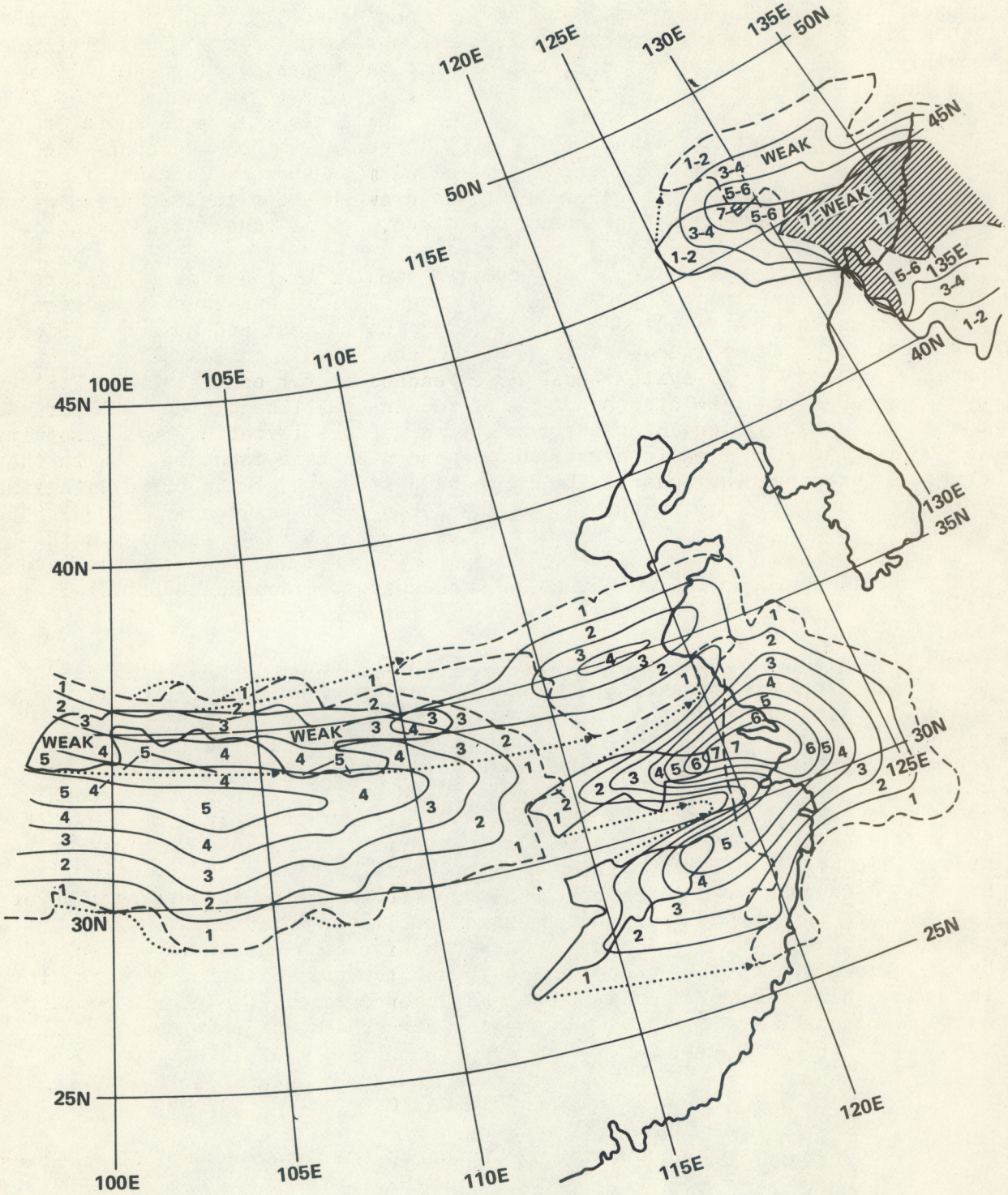


Figure 13.--Workmap, China, for the period 9 a.m. to 8 p.m., local time, March 10, 1975

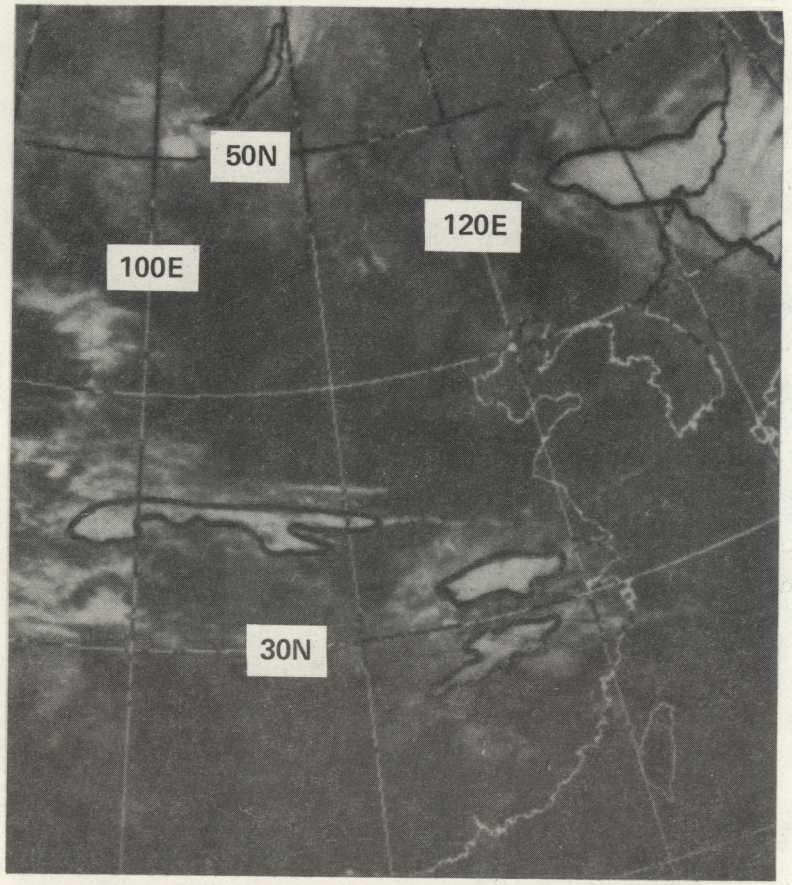


Figure 14.--Infrared imagery taken at approximately 9 a.m., local time, March 10, 1975, over Asia.

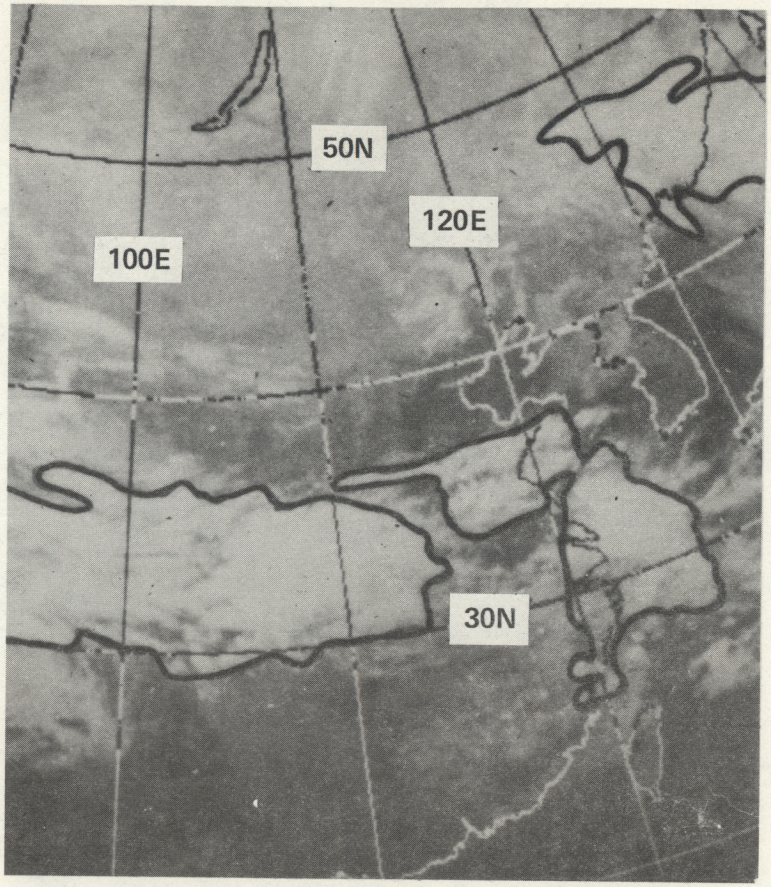


Figure 15.--Infrared imagery taken at approximately 8 p.m., local time, March 10, 1975, over Asia.

| 12-hour period number | Grid point number | | | | | | | | | | | | | | |
|---|---|---|---|---|---|---|---|---|---|---|---|---|---|---|---|
| | 1 | 2 | 3 | 4 | 5 | 6 | 7 | 8 | 9 | 10 | 11 | 12 | 13 | 14 | 15 |
| 1 | 2 | 3 | 4 | 3 | 2 | 1 | | | | | 6 | 6 | 5 | 4 | 3 |
| 2 | 1 | 4 | 6 | 9 | 8 | 5 | 3 | | | | 1 | 5 | 8 | 9 | 9 |
| 3 | | | | 1 | 3 | 5 | 8 | 5 | | | | | | 2 | 4 |
| 4 | 1 | | | | | | | 2 | | | | | | | |
| 5 | 9 | 7 | 5 | 2 | 1 | | | | | | 7 | 5 | 4 | 2 | |
| 6 | 8 | 8 | 9 | 8 | 4 | | | | | | 9 | 8 | 7 | 4 | |
| 7 | 4 | 7 | 9 | 8 | 8 | 6 | 4 | 2 | | | 9 | 8 | 8 | 7 | 7 |
| 8 | 3 | 9 | 9 | 9 | 8 | 6 | 6 | 8 | 8 | 8 | 2 | 7 | 9 | 7 | 9 |
| 9 | 1 | 1 | 2 | 3 | 2 | 1 | 5 | 9 | | | | | 1 | 1 | 1 |
| 10 | | 1 | | | | | | | | 9 | | | | | |
| 11 | 7 | 6 | 5 | 4 | 3 | 2 | | | | 2 | 7 | 6 | 5 | 4 | 2 |
| 12 | | 6 | 8 | 9 | 9 | 8 | | | | | | 3 | 9 | 8 | 9 |
| 13 | 3 | 2 | 2 | 5 | 8 | 8 | 4 | | | | | | 2 | 4 | 7 |
| 14 | 1 | 1 | | | | 4 | 9 | 6 | | 1 | | | | | |
| Total | 40 | 55 | 59 | 61 | 56 | 46 | 39 | 32 | 8 | 20 | 41 | 48 | 58 | 52 | 51 |
| Normal | 0.06 | 0.07 | 0.07 | 0.06 | 0.06 | 0.07 | 0.09 | 0.10 | 0.10 | 0.12 | 0.05 | 0.07 | 0.09 | 0.08 | 0.06 |
| Est. | .02 | .04 | .04 | .04 | .03 | .03 | .04 | .03 | .01 | .02 | .02 | .03 | .05 | .04 | .03 |

Figure 16.--Data sheet for grid points 1 through 15 (China) for the week, March 16-22, 1975.

became available) and were completed on April 21. The April estimates were completed on April 21. The April estimates were completed at a more leisurely pace. Figures 17 and 18 are examples of weekly precipitation estimates. Figure 19 shows the number of consecutive days in April for which no precipitation was estimated at various USSR grid points. This statistic is important for agricultural planning.

Precipitation data over the USSR were available for verification, although much was of questionable quality. No Chinese precipitation data were available.

For the 4-week period, March 2-29, 1975, total observed precipitation was determined for each reporting point in the parts of the USSR under study. The total for each reporting point was compared with the 4-week estimate at the nearest grid point. The mean absolute error was 55% of the mean observed precipitation. Bias, however, was virtually zero.

The technique was tested over the central United States for April 1976. Daily estimates were made for 547 rain reporting points in the 24 states lying between the Rockies and the Appalachians. Estimates were made for individual stations rather than for grid points to make use of excellent climatological normals and daily reports afforded by the stations used in the sample.

Because of picture-taking times of the polar-orbiting satellite, NOAA-4, the estimates cover the period from 8 p.m. to 8 p.m., local time, approximately. If all reporting points took observations at 8 p.m., local time, verification of the technique would be greatly facilitated. Unfortunately for this study, only 1 to 2% of the readings received by the Environmental Data Service for publication in the *Climatological Data* are taken at this time. Therefore, in selecting the verification sample, the primary data sources chosen are the National Weather Service and Federal Aviation Administration stations, which take rainfall measurements at midnight local standard time. The secondary source is a group of climatological and river-rainfall stations taking observations between 4 p.m. and 8 p.m., local standard time; these stations fill the gaps in the primary network. In areas devoid of such points, a few stations that take morning or early afternoon observations have been added to the sample. However, the time discrepancies thus introduced perhaps may have been too great a price to pay for the increase in geographical coverage.

Of the several verification checks applied to the United States estimates for April 1976, all but one show more accurate estimates for the primary source stations (NWS and FAA) than for the sample as a whole.

The grand total of *daily* errors (disregarding sign) for all stations for the entire month has been divided by the grand total of observed precipitation. The ratio for the entire sample is 1.00, and for the primary source stations, 0.96. Similar ratios have been calculated for each station. The median ratio for the entire sample is 0.98, and for the primary source stations, 0.95.

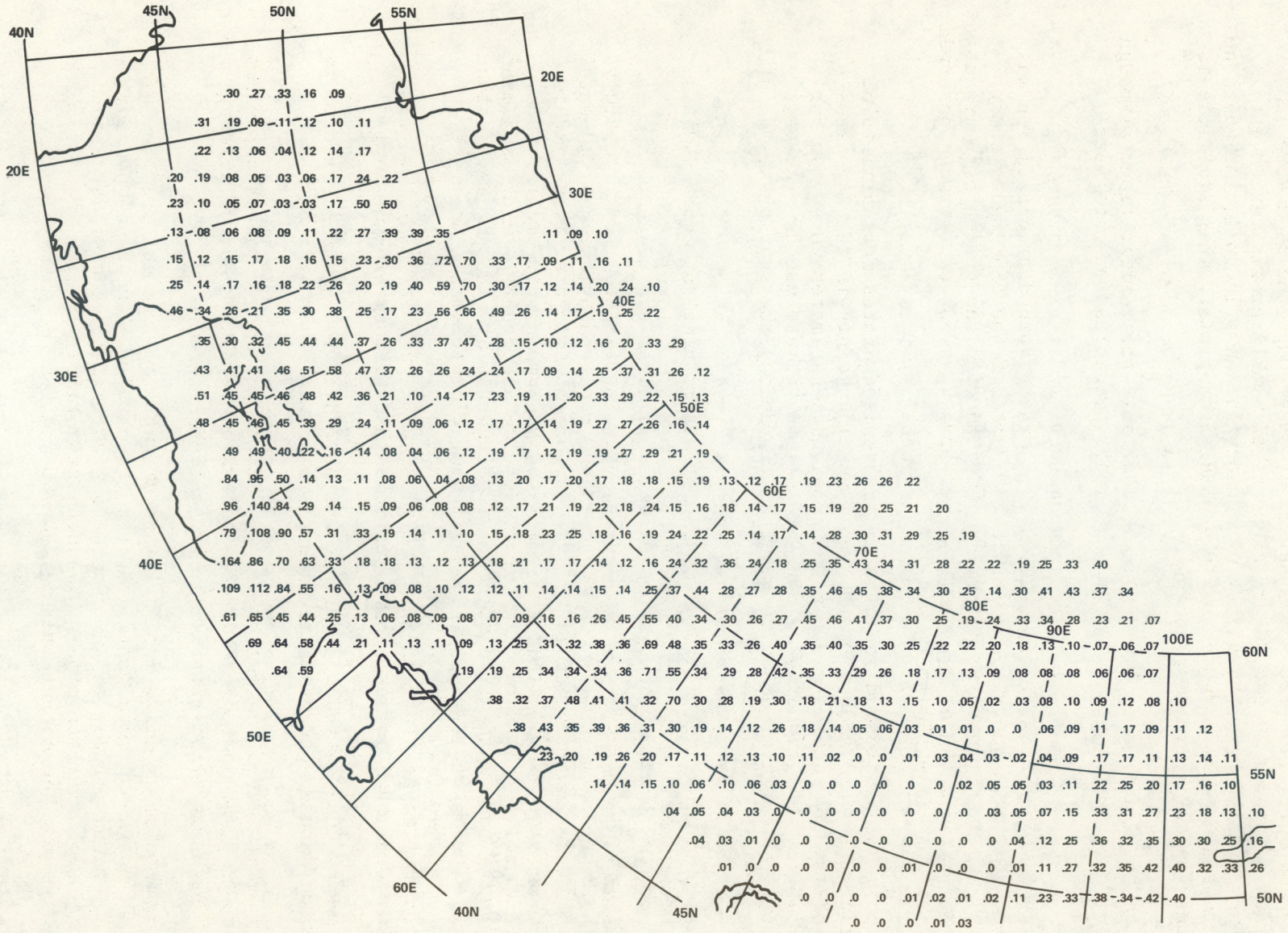


Figure 17.--Weekly precipitation estimates in hundredths of an inch for the USSR for April 13 to 19, 1975, inclusive.

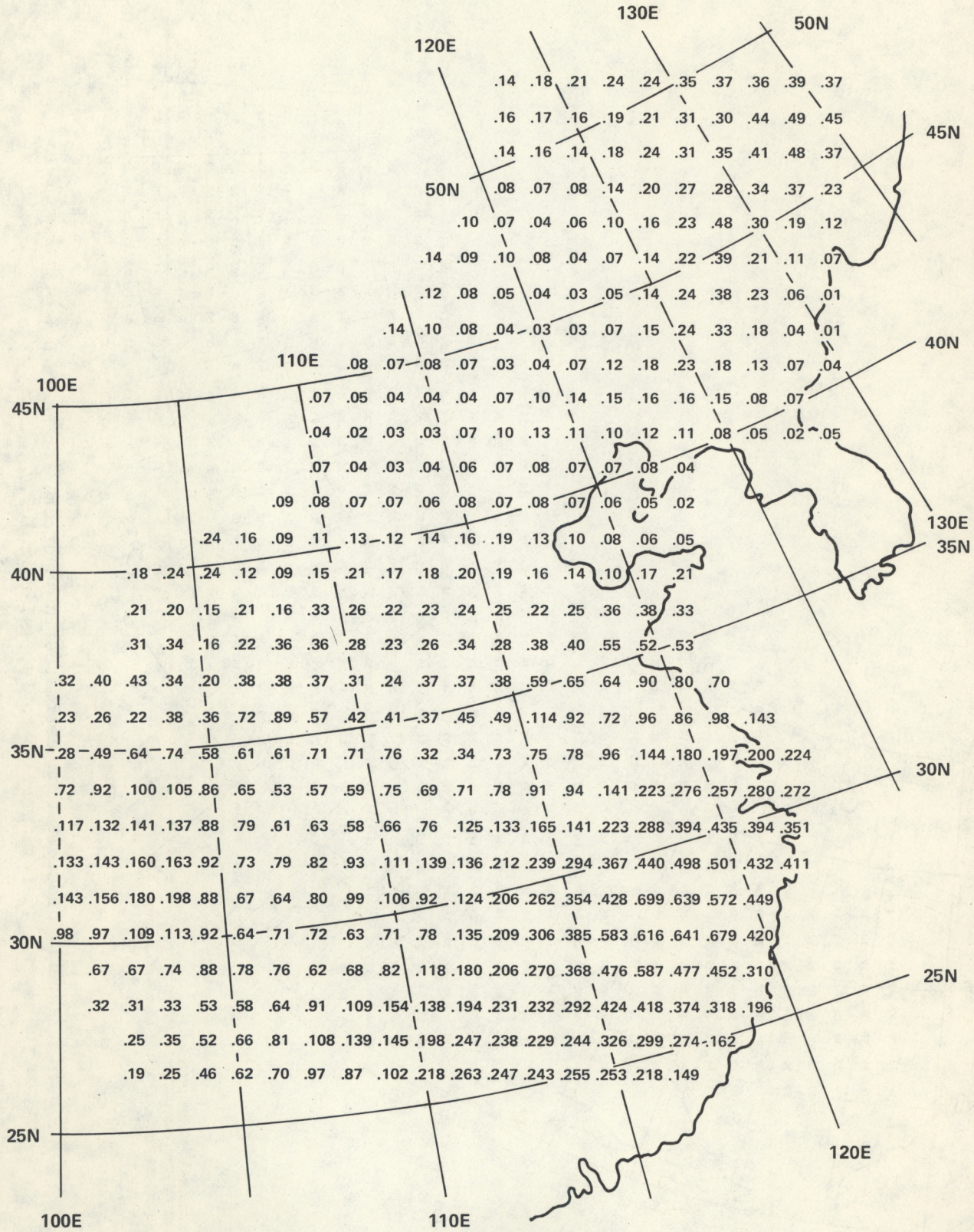


Figure 18.--Weekly precipitation estimates in hundredths of an inch for China for April 13 to 19, 1975, inclusive.

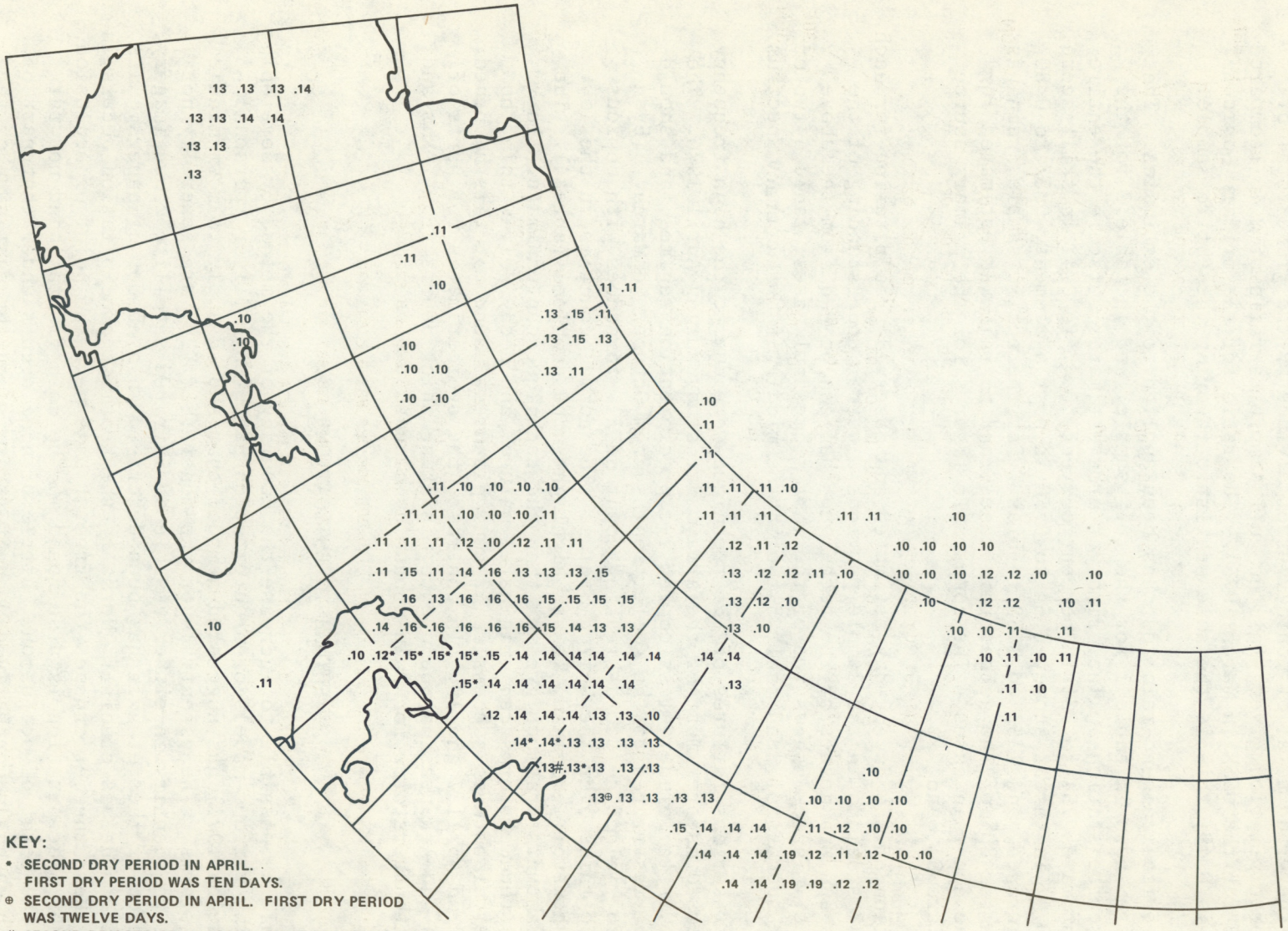


Figure 19.--Number of consecutive days in April 1975 for which no precipitation was estimated at USSR grid points.

The above ratios are based on daily errors, a rigorous test. The ratio of *monthly* error to total monthly precipitation is far less exact, but useful. The grand total of monthly error divided by the grand total of monthly precipitation gives, for the full sample, a ratio of 0.46 (compared with 0.55 for the USSR in March 1975). The ratio for the primary source stations is 0.49; this is the sole statistic favoring the entire sample.

A categorical rain-no-rain test has been applied to the estimates. The results are shown in table 1 for the full sample, and in table 2 for the primary source stations. The primary source estimates outscore the entire sample estimates 75% to 73% in percent correct, 0.47 to 0.42 in skill score, 0.49 to 0.45 in threat score, 0.54 to 0.50 in post agreement, 0.83 to 0.80 in prefigurance, and 1.53 to 1.58 in bias. For the entire sample, rain was estimated for 80% of the actual rain cases, and no rain was estimated for 70% of the non-rain cases. The comparable figures for the primary source stations are 83% and 71%.

Inspection of the day-by-day estimated and observed precipitation for each of the 547 stations in the sample provides a better understanding of the strengths and weaknesses of the technique than can be had from the above statistics. Table 3 shows two of the most successful cases, table 4 two of the least successful, and table 5 two in the middle of the accuracy spectrum.

The most serious failures of the technique were due to the high frequency of thunderstorms over most of the area under study during April 1976. The technique is tailored to less convective precipitation regimes, and should perhaps be restricted to the cooler months from October to March. (Even March 1976 yielded a record-breaking count of 211 tornadoes with copious convective rains over the United States. The normal count is in the low forties, however.) Goliad, Texas, highlights the problem (table 4). The observed amounts are much greater than the technique can estimate. In addition, thunderstorms can originate, mature, and decay well within the time interval between successive 12-hour pictures. No doubt this happened at Goliad on April 7 and 19. In contrast, the overestimates for parts of Louisiana and Arkansas may be due to mistaking thick debris from Texas and Oklahoma thunderstorms for rain-producing clouds.

## FUTURE INVESTIGATIONS

It should be possible to increase the accuracy of the method by developing or adapting various models of precipitation patterns. Oliver (personal communication 1974) has suggested a model that should apply to most middle latitude storms. The essentials of the model (Fig. 20) are generally not difficult to identify in either visible or infrared satellite cloud imagery. The location of the jet axis has been described in a number of papers. Its role in the model is crucial. Normally the heaviest precipitation occurs in the area where the jet crosses the frontal band near the point of occlusion. Significant precipitation is also found in the cold frontal band not far south of the point of occlusion. Little or none occurs under that part of the jet which has a northerly component (that is, on the east side of the upper level ridge line).

Table 1.--Categorical rain-no rain verification of estimates for 547 stations over central United States.

| | | Estimated | | |
|---|---|---|---|---|
| | | Rain | None | Total |
| Observed | Rain | 3612 ($a$) | 907 ($b$) | 4519 ($a$) |
| | None | 3542 ($c$) | 8349 ($d$) | 11891 ($c+d$) |
| | Total | 7154 ($a+c$) | 9256 ($b+d$) | 16410 ($a+b+c+d$) |

Total cases ($T$) = 16410

Total correct ($R$) = 11961

Percent correct = 73%

Expected correct by chance ($E$)

$$= \frac{(a+b)(a+c)+(c+d)(b+d)}{T} = \frac{(4519)(7154)+(11891)(9256)}{16410} = 8677$$

$$\text{Skill score} = \frac{R-E}{T-E} = \frac{11961-8677}{16410-8677} = .42$$

$$\text{Threat score} = \frac{3612}{3612+907+3542} = .45$$

$$\text{Post agreement} = \frac{3612}{7154} = .50$$

$$\text{Prefigurance} = \frac{3612}{4519} = .80$$

$$\text{Bias} = \frac{7154}{4519} = 1.58$$

Table 2.--Categorical rain-no rain verification of estimates for first order and airport stations (162).

| | | Estimated | | |
|---|---|---|---|---|
| | | Rain | None | Total |
| Observed | Rain | 1185 ($a$) | 243 ($b$) | 1428 ($a+b$) |
| | None | 996 ($c$) | 2436 ($d$) | 3432 ($c+d$) |
| | Total | 2181 ($a+c$) | 2679 ($b+d$) | 4860 ($a+b+c+d$) |

Total cases ($T$) = 4860

Total correct ($R$) = 3621

Percent correct = 75%

Expected correct by chance ($E$)

$$= \frac{(1428)(2181)+(3432)(2679)}{4860} = 2533$$

$$\text{Skill score} = \frac{R-E}{T-E} = \frac{3621-2533}{4860-2533} = .47$$

$$\text{Threat score} = \frac{1185}{1185+243+996} = .49$$

$$\text{Post agreement} = \frac{1185}{2181} = .54$$

$$\text{Prefigurance} = \frac{1185}{1428} = .83$$

$$\text{Bias} = \frac{2181}{1428} = 1.53$$

Table 3.--Estimated and observed daily rainfall for selected stations in the United States, April 1976. (Best cases.)

| | Youngstown, Ohio | | | Rockford, Illinois | | |
|---|---|---|---|---|---|---|
| 1976 | Est | Obs | E-O | Est | Obs | E-O |
| April 1 | 0.07 | 0.10 | -0.03 | 0.04 | T | +0.04 |
| 2 | .04 | .04 | 0 | 0 | 0 | 0 |
| 3 | 0 | 0 | 0 | 0 | .04 | -.04 |
| 4 | .07 | .17 | -.10 | 0 | .03 | -.03 |
| 5 | 0 | 0 | 0 | 0 | 0 | 0 |
| 6 | .04 | .01 | +.03 | 0 | 0 | 0 |
| 7 | 0 | .04 | -.04 | 0 | 0 | 0 |
| 8 | 0 | T | 0 | 0 | 0 | 0 |
| 9 | 0 | 0 | 0 | 0 | 0 | 0 |
| 10 | 0 | 0 | 0 | .04 | .16 | -.12 |
| 11 | .04 | .03 | +.01 | .08 | .05 | +.03 |
| 12 | 0 | 0 | 0 | 0 | 0 | 0 |
| 13 | 0 | 0 | 0 | 0 | 0 | 0 |
| 14 | 0 | 0 | 0 | 0 | 0 | 0 |
| 15 | 0 | 0 | 0 | .35 | .86 | -.51 |
| 16 | .04 | .04 | 0 | .12 | T | +.12 |
| 17 | .04 | 0 | +.04 | .08 | .04 | +.04 |
| 18 | 0 | 0 | 0 | .12 | .02 | +.10 |
| 19 | 0 | 0 | 0 | 0 | 0 | 0 |
| 20 | 0 | 0 | 0 | .19 | .51 | -.32 |
| 21 | .29 | .38 | -.09 | .35 | .35 | 0 |
| 22 | .11 | .32 | -.21 | 0 | 0 | 0 |
| 23 | .04 | 0 | +.04 | .38 | .50 | -.12 |
| 24 | .18 | .17 | +.01 | .62 | .75 | -.13 |
| 25 | .40 | .26 | +.14 | .35 | .17 | +.18 |
| 26 | .04 | .08 | -.04 | 0 | 0 | 0 |
| 27 | 0 | T | 0 | 0 | 0 | 0 |
| 28 | 0 | 0 | 0 | 0 | 0 | 0 |
| 29 | 0 | 0 | 0 | 0 | 0 | 0 |
| 30 | 0 | 0 | 0 | .08 | .12 | -.04 |
| Total | 1.40 | 1.64 | 0.78* | 2.80 | 3.60 | 1.82* |
| Ratio: | 0.48 | | -0.24# | Ratio: | 0.51 | -0.80# |

*Total of daily errors, disregarding sign.

#Algebraic sum of daily errors, which equals total estimated minus total observed.

Table 4.--Estimated and observed daily rainfall for selected stations in the United States, April 1976. (Worst cases.)

| 1976 | Jennings, Louisiana Est | Obs | E-O | Goliad, Texas Est | Obs | E-O |
|---|---|---|---|---|---|---|
| April 1 | 0 | 0 | 0 | 0.03 | 0 | +0.03 |
| 2 | 0 | 0 | 0 | .13 | 0 | +.13 |
| 3 | 0 | 0 | 0 | 0 | 0 | 0 |
| 4 | 0 | 0 | 0 | .42 | .31 | +.11 |
| 5 | .87 | 0 | +.87 | .03 | 1.18 | -1.15 |
| 6 | .27 | .07 | +.20 | .16 | 0 | +.16 |
| 7 | .38 | 0 | +.38 | .18 | .08 | +.10 |
| 8 | 0 | .05 | -.05 | 0 | 1.75 | -1.75 |
| 9 | 0 | 0 | 0 | .03 | 0 | +.03 |
| 10 | 0 | 0 | 0 | 0 | 0 | 0 |
| 11 | 0 | 0 | 0 | 0 | 0 | 0 |
| 12 | 0 | 0 | 0 | .05 | T | +.05 |
| 13 | .33 | 0 | +.33 | .10 | .17 | -.07 |
| 14 | 0 | .02 | -.02 | .03 | 0 | +.03 |
| 15 | .16 | 0 | +.16 | .08 | 0 | +.08 |
| 16 | .11 | 0 | +.11 | 0 | .39 | -.39 |
| 17 | 0 | 0 | 0 | 0 | 0 | 0 |
| 18 | 0 | 0 | 0 | .23 | 5.00 | -4.77 |
| 19 | 0 | 0 | 0 | 0 | 3.35 | -3.35 |
| 20 | .27 | 0 | +.27 | .16 | .72 | -.56 |
| 21 | 0 | .42 | -.42 | 0 | 0 | 0 |
| 22 | 0 | 0 | 0 | .03 | 0 | +.03 |
| 23 | 0 | 0 | 0 | .16 | 0 | +.16 |
| 24 | .27 | 0 | +.27 | .42 | 0 | +.42 |
| 25 | .11 | .30 | -.19 | .13 | .15 | -.02 |
| 26 | 0 | 0 | 0 | 0 | 0 | 0 |
| 27 | 0 | 0 | 0 | 0 | 0 | 0 |
| 28 | 0 | 0 | 0 | .10 | .01 | +.09 |
| 29 | .49 | 0 | +.49 | .31 | 1.11 | -.80 |
| 30 | .16 | 0 | +.16 | .03 | .01 | +.02 |
| Total | 3.42 | 0.86 | 3.92* | 2.81 | 14.23 | 14.30* |
| Ratio: | 4.56 | | +2.56# | Ratio: | 1.00 | -11.42# |

*Total of daily errors, disregarding sign.

#Algebraic sum of daily errors, which equals total estimated minus total observed.

Table 5.--Estimated and observed daily rainfall for selected stations in the United States, April 1976. (Average cases.)

| 1976 | Ridgeland, Wisconsin Est | Obs | E-O | Cherokee, Oklahoma Est | Obs | E-O |
|---|---|---|---|---|---|---|
| April 1 | 0 | 0 | 0 | 0 | 0 | 0 |
| 2 | 0 | 0 | 0 | 0 | 0 | 0 |
| 3 | .09 | T | +.09 | 0 | 0 | 0 |
| 4 | 0 | 0 | 0 | 0 | 0 | 0 |
| 5 | 0 | 0 | 0 | 0 | 0 | 0 |
| 6 | 0 | 0 | 0 | 0 | 0 | 0 |
| 7 | 0 | 0 | 0 | .21 | T | +.21 |
| 8 | 0 | 0 | 0 | 0 | 0 | 0 |
| 9 | .03 | 0 | +.03 | 0 | 0 | 0 |
| 10 | .11 | .22 | -.11 | .30 | .02 | +.28 |
| 11 | 0 | 0 | 0 | .03 | 0 | +.03 |
| 12 | 0 | 0 | 0 | 0 | .46 | -.46 |
| 13 | 0 | 0 | 0 | 0 | 0 | 0 |
| 14 | .03 | .69 | -.66 | 0 | 0 | 0 |
| 15 | .03 | 0 | +.03 | .09 | T | +.09 |
| 16 | .09 | 0 | +.09 | .18 | .69 | -.51 |
| 17 | .20 | .04 | +.16 | .06 | .60 | -.54 |
| 18 | 0 | .90 | -.90 | 0 | 0 | 0 |
| 19 | 0 | 0 | 0 | .15 | 0 | +.15 |
| 20 | .09 | 0 | +.09 | .30 | .59 | -.29 |
| 21 | .26 | .26 | 0 | 0 | 0 | 0 |
| 22 | .03 | .01 | +.02 | 0 | 0 | 0 |
| 23 | .09 | .24 | -.15 | .06 | 0 | +.06 |
| 24 | .40 | .27 | +.13 | .09 | .20 | -.11 |
| 25 | .11 | 0 | +.11 | 0 | 0 | 0 |
| 26 | 0 | 0 | 0 | .06 | T | +.06 |
| 27 | 0 | 0 | 0 | .09 | T | +.09 |
| 28 | 0 | 0 | 0 | .36 | .91 | -.55 |
| 29 | 0 | 0 | 0 | 0 | 0 | 0 |
| 30 | 0 | T | 0 | .12 | .34 | -.22 |
| Total | 1.56 | 2.63 | 2.57* | 2.10 | 3.81 | 3.65* |
| Ratio: | 0.98 | | -1.07# | Ratio: | 0.96 | -1.71# |

*Total of daily errors, disregarding sign.

#Algebraic sum of daily errors, which equals total estimated minus total observed.

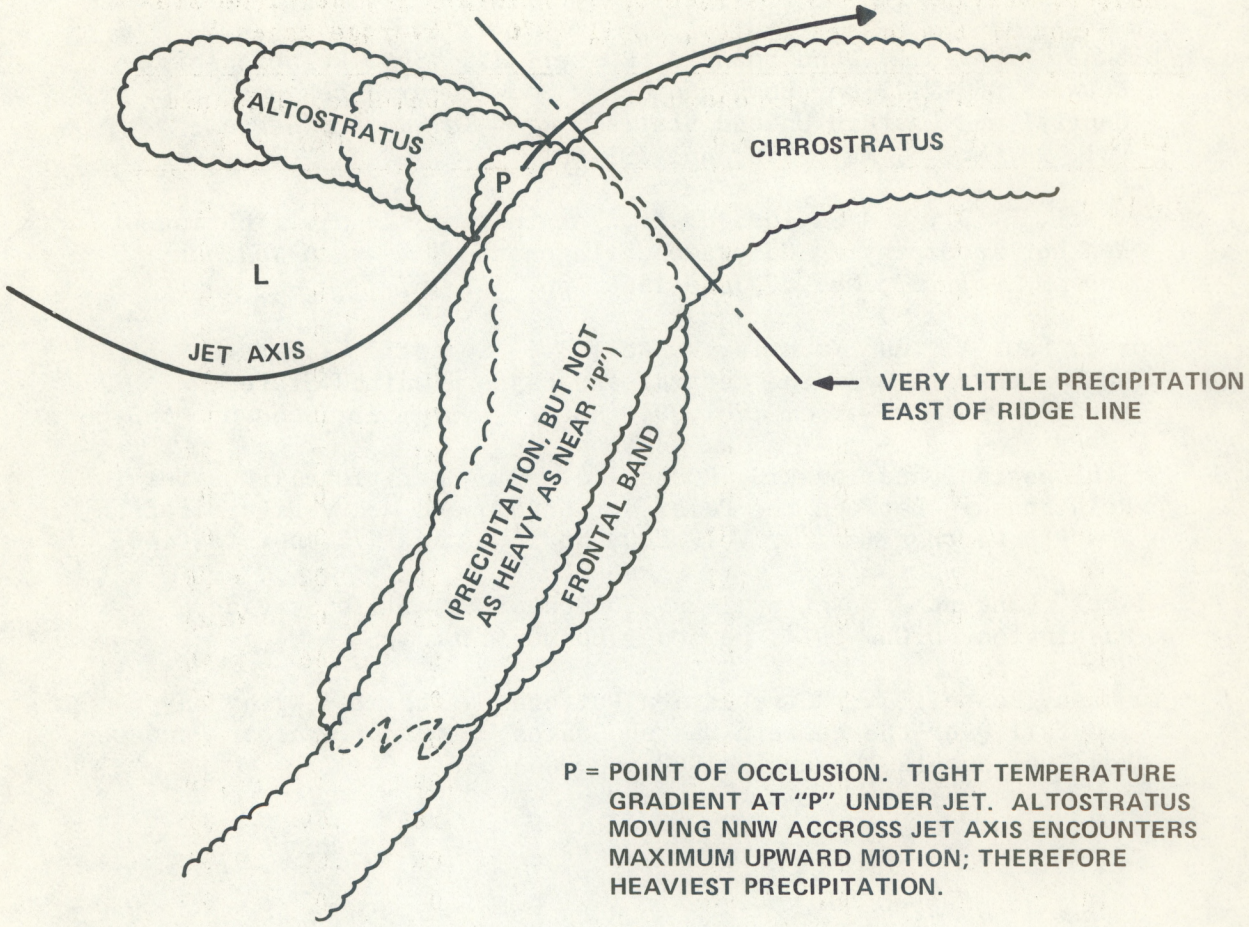


Figure 20.--Middle-latitude storm model showing zones of greatest intensity of precipitation (from Oliver).

Smith and Younkin (1972) have shown that for "digging" polar jets over the central United States, heavy rainfall tends to occur in an ellipsoidal pattern east of the jet stream. Their composite model for forecasting 12-hour heavy rainfall should be tested, both over the central United States and other parts of the globe, for possible use in this technique. Other investigations by Younkin and his collaborators (1968, 1970) and by Fawcett and Saylor (1965) should be tested in the same way.

## ACKNOWLEDGMENTS

The author wishes to thank Vincent J. Oliver and Dr. Norton D. Strommen for valuable suggestions for improving the paper; Paul Lehr for his editorial review; and Peg Follansbee, his personal secretary, who helped so much.

## REFERENCES

Browne, Richard F., and Younkin, Russell J., "Some Relationships Between 850-Millibar Lows and Heavy Snow Occurrences Over the Central and Eastern United States," *Monthly Weather Review*, Vol. 98, No. 5, May 1970, pp. 399-401.

Fawcett, E. B., and Saylor, H. K., "A Study of the Distribution of Weather Accompanying Colorado Cyclogenesis," *Monthly Weather Review*, Vol. 93, No. 6, June 1965, pp. 359-367.

Goree, Paul A., and Younkin, Russell J., "Synoptic Climatology of Heavy Snowfall Over the Central and Eastern United States," *Monthly Weather Review*, Vol. 94, No. 11, November 1966, pp. 663-668.

Smith, Warren, and Younkin, Russell J., "An Operationally Useful Relationship Between the Polar Jet Stream and Heavy Precipitation," *Monthly Weather Review*, Vol. 100, No. 6, June 1972, pp. 434-440.

Oliver, Vincent J., National Environmental Satellite Service, Washington, D.C., 1974, personal communication.

Younkin, Russell J., "Circulation Patterns Associated With Heavy Snowfall Over the Western United States," *Monthly Weather Review*, Vol. 96, No. 12, December 1968, pp. 851-853.

(Continued from inside front cover)

NESS 59 Use of Geostationary-Satellite Cloud Vectors to Estimate Tropical Cyclone Intensity. Carl. O. Erickson, September 1974, 37 pp. (COM-74-11762/AS)

NESS 60 The Operation of the NOAA Polar Satellite System. Joseph J. Fortuna and Larry N. Hambrick, November 1974, 127 pp. (COM-75-10390/AS)

NESS 61 Potential Value of Earth Satellite Measurements to Oceanographic Research in the Southern Ocean. E. Paul McClain, January 1975, 18 pp. (COM-75-10479/AS)

NESS 62 A Comparison of Infrared Imagery and Video Pictures in the Estimation of Daily Rainfall From Satellite Data. Walton A. Follansbee and Vincent J. Oliver, January 1975, 14 pp. (COM-75-10435/AS)

NESS 63 Snow Depth and Snow Extent Using VHRR Data From the NOAA-2 Satellite. David F. McGinnis, Jr., John A. Pritchard, and Donald R. Wiesnet, February 1975, 10 pp. (COM-75-10482/AS)

NESS 64 Central Processing and Analysis of Geostationary Satellite Data. Charles F. Bristor (Editor), March 1975, 155 pp. (COM-75-10853/AS)

NESS 65 Geographical Relations Between a Satellite and a Point Viewed Perpendicular to the Satellite Velocity Vector (Side Scan). Irwin Ruff and Arnold Gruber, March 1975, 14 pp. (COM-75-10678/AS) 10678/AS)

NESS 66 A Summary of the Radiometric Technology Model of the Ocean Surface in the Microwave Region. John C. Alishouse, March 1975, 24 pp. (COM-75-10849/AS)

NESS 67 Data Collection System Geostationary Operational Environmental Satellite: Preliminary Report. Merle L. Nelson, March 1975, 48 pp. (COM-75-10679/AS)

NESS 68 Atlantic Tropical Cyclone Classifications for 1974. Donald C. Gaby, Donald R. Cochran, James B. Lushine, Samuel C. Pearce, Arthur C. Pike, and Kenneth O. Poteat, April 1975, 6 pp. (COM-75-1-676/AS)

NESS 69 Publications and Final Reports on Contracts and Grants, NESS-1974. April 1975, 7 pp. (COM-75-10850/AS)

NESS 70 Dependence of VTPR Transmittance Profiles and Observed Radiances on Spectral Line Shape Parameters. Charles Braun, July 1975, 17 pp.

NESS 71 Nimbus-5 Sounder Data Processing System, Part II: Results. W. L. Smith, H. M. Woolf, C. M. Hayden, and W. C. Shen. July 1975, 102 pp.

NESS 72 Radiation Budget Data From the Meteorological Satellites, ITOS 1 and NOAA 1. Donald H. Flanders and William L. Smith, August 1975, 22 pp.

NESS 73 Operational Processing of Solar Proton Monitor Data. Stanley R. Brown, September 1975. (Revision of NOAA TM NESS 49), 15 pp.

NESS 74 Monthly Winter Snowline Variation in the Northern Hemisphere from Satellite Records, 1966-75. Donald R. Wiesnet and Michael Matson, November 1975, 21 pp. (PB248437)

NESS 75 Atlantic Tropical and Subtropical Cyclone Classifications for 1975. D. C. Gaby, J. B. Lushine, B. M. Mayfield, S. C. Pearce, and K. O. Poteat, March, 1976, 14 pp.

NESS 76 The Use of the Radiosonde in Deriving Temperature Soundings From the Nimbus and NOAA Satellite Data. Christopher M. Hayden, April 1976, 21 pp. (PB-256755)

NESS 77 Algorithm for Correcting the VHRR Imagery for Geometric Distortions Due to the Earth's Curvature and Rotation. Richard Legeckis and John Pritchard, April 1976, 30 pp.

NESS 78 Satellite Derived Sea-Surface Temperatures From NOAA Spacecraft. Robert L. Brower, Hilda S. Gohrband, William G. Pichel, T. L. Signore, and Charles C. Walton, in press, 1975.

NESS 79 Publications and Final Reports on Contracts and Grants, 1975. NESS, June 1976.

NESS 80 Satellite Images of Lake Erie Ice: January-March 1975. Michael C. McMillan and David Forsyth, June 1976.